AD-A172 711 PRESSURE INTERACTIONS IN SUPERSONIC COMBUSTION(U) 1/1
SCIENCE APPLICATIONS INTERNATIONAL CORP CHATSWORTH CA
COMBUST.. R B EDELMAN ET AL. 11 JUN 86
UNCLASSIFIED AFOSR-TR-86-0876 F49620-84-C-0064 F/G 21/2 NL

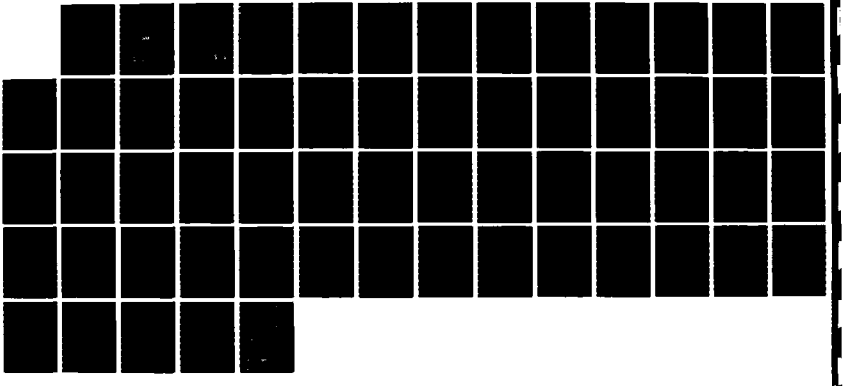

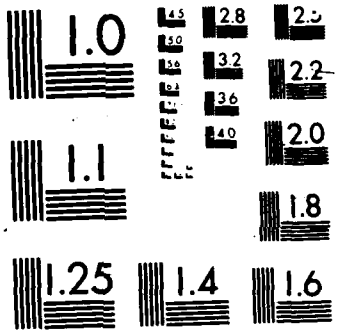
1.0
1.1
1.25
1.4
1.6
1.8
2.0
2.2
2.8
3.2
3.6
4.0

AFOSR-TR- 86-0876

(2)

AD-A172 711

PRESSURE INTERACTIONS IN SUPERSONIC COMBUSTION

FINAL REPORT

AIR FORCE OFFICE OF SCIENTIFIC RESEARCH (AFSC)
NOTICE OF TRANSMITTAL TO DTIC
This technical report has been reviewed and is
approved for public release IAW AFR 190-12.
Distribution is unlimited.
MATTHEW J. KELLY
Chief, Technical Information Division

SAIC™

Science Applications International Corporation

DTIC FILE COPY

DTIC
ELECTE
OCT 0 8 1986
S D
D

Approved for public release;
distribution unlimited.

(2)

SAIC 86/1739

AFOSR-TR- 86-0876

PRESSURE INTERACTIONS IN SUPERSONIC COMBUSTION

FINAL REPORT

SUBMITTED BY:

SCIENCE APPLICATIONS INTERNATIONAL CORPORATION

COMBUSTION SCIENCE AND ADVANCED TECHNOLOGY DEPARTMENT

9760 Owensmouth Avenue

Chatsworth, California 91311

Contract No. F49620-84-C-0064

PREPARED FOR:

AIR FORCE OFFICE OF SCIENTIFIC RESEARCH

BOLLING AIR FORCE BASE

Washington, D.C. 20332

June 11, 1986

SAIC

AD-A172 [illegible]

REPORT DOCUMENTATION PAGE

1a. REPORT SECURITY CLASSIFICATION: Unclassified	1b. RESTRICTIVE MARKINGS: None
2a. SECURITY CLASSIFICATION AUTHORITY	3. DISTRIBUTION/AVAILABILITY OF REPORT: Distribution unlimited; approved for public release
2b. DECLASSIFICATION/DOWNGRADING SCHEDULE	
4. PERFORMING ORGANIZATION REPORT NUMBER(S)	5. MONITORING ORGANIZATION REPORT NUMBER(S): AFOSR-TR- 86-0876
6a. NAME OF PERFORMING ORGANIZATION: Science Applications International Corporation; 6b. OFFICE SYMBOL (If applicable):	7a. NAME OF MONITORING ORGANIZATION: Air Force Office of Scientific Research
6c. ADDRESS (City, State and ZIP Code): 9760 Owensmouth Ave.,Chatsworth,CA 91311	7b. ADDRESS (City, State and ZIP Code): Bolling AFB DC 20332-6448
8a. NAME OF FUNDING/SPONSORING ORGANIZATION: Air Force Office of Sci.Res.; 8b. OFFICE SYMBOL (If applicable): AFOSR/NA	9. PROCUREMENT INSTRUMENT IDENTIFICATION NUMBER: F49620-84-C-0064
8c. ADDRESS (City, State and ZIP Code): Bolling AFB DC 20332-6448	10. SOURCE OF FUNDING NOS.

PROGRAM ELEMENT NO.	PROJECT NO.	TASK NO.	WORK UNIT NO.
61102F	2308	A2	

11. TITLE (Include Security Classification): Pressure Interactions in Supersonic Comb.(Unc).

12. PERSONAL AUTHOR(S): R.B.Edelman and W.N.Bragg

13a. TYPE OF REPORT	13b. TIME COVERED	14. DATE OF REPORT (Yr., Mo., Day)	15. PAGE COUNT
Final	FROM 1 JUN 84 TO 28 Feb86	1986, June 11	55

16. SUPPLEMENTARY NOTATION

17. COSATI CODES			18. SUBJECT TERMS (Continue on reverse if necessary and identify by block number)
FIELD	GROUP	SUB. GR.	Supersonic Combustion, Sudden Expansion ~~(Dump)~~ Combustors, Pressure Interactions, Modular Model Computer Code, Turbulence Modeling, [illegible] Combustors.

19. ABSTRACT (Continue on reverse if necessary and identify by block number)

A detailed assessment of supersonic combustion has been carried out to identify specific research requirements in modeling turbulent reacting supersonic flows. The direct effects of pressure gradients and pressure fluctuations on turbulence were found to be potentially responsible for certain of the trends in turbulent transport and mixing rates that are observed in supersonic flows. An approach to the modeling of these phenomena is delineated. A modular model computer code for the analysis of sudden expansion (dump) combustors was prepared and delivered to the Air Force Aero Propulsion Laboratories (AFWAL/PORT). This modular model is designed to be used parametrically in evaluating effects such as chemical kinetics limitation on flame stabilization and combustion efficiency in integral rocket ramjet and ducted rocket combustors.

20. DISTRIBUTION/AVAILABILITY OF ABSTRACT	21. ABSTRACT SECURITY CLASSIFICATION
UNCLASSIFIED/UNLIMITED ☒ SAME AS RPT. ☐ DTIC USERS ☐	Unclassified

22a. NAME OF RESPONSIBLE INDIVIDUAL	22b. TELEPHONE NUMBER (Include Area Code)	22c. OFFICE SYMBOL
Julian M. Tishkoff	(202) 767-4935	AFOSR/NA

DD FORM 1473, 83 APR — EDITION OF 1 JAN 73 IS OBSOLETE.

Unclassified
SECURITY CLASSIFICATION OF THIS PAGE

TABLE OF CONTENTS

LIST OF FIGURES

LIST OF SYMBOLS

SYMBOL	DESCRIPTION
a	SPEED OF SOUND
C_i	CONSTANT
C_p	CONSTANT PRESSURE SPECIFIC HEAT
D_{ij}	DIFFUSION COEFFICIENT
h	STATIC ENTHALPY
H	TOTAL ENTHALPY
j_i	DIFFUSIONAL FLUX OF THE i^{th} SPECIE
k, e	TURBULENT KINETIC ENERGY
ℓ	COORDINATE ALONG A CHARACTERISTIC
Le	LEWIS NUMBER
M	MACH NUMBER
n	COORDINATE NORMAL TO THE STREAMLINE
p	PRESSURE
Pr	PRANDTL NUMBER
q	MAGNITUDE OF THE VELOCITY VECTOR
r	RADIAL COORDINATE
R	UNIVERSAL GAS CONSTANT
s	COORDINATE ALONG THE STREAMLINE
T	TEMPERATURE
u	AXIAL VELOCITY
$\underline{V}$	VELOCITY VECTOR
$\dot{W}_i$	PRODUCTION RATE OF THE i^{th} SPECIES DUE TO CHEMICAL REACTIONS

LIST OF SYMBOLS

SYMBOL	DESCRIPTION
X	STREAMWISE COORDINATE
Y	LATERAL COORDINATE
a_i	MASS FRACTION OF THE i^{th} SPECIE
δ_{ij}	KRONECKER'S DELTA
ϵ	DISSIPATION RATE OR ANGLE
γ	SPECIFIC HEAT RATIO
ρ	DENSITY
σ	SPREAD RATE PARAMETER
θ	STREAMLINE DIRECTION RELATIVE TO THE HORIZONTAL DIRECTION
$\underline{\tau}$	VISCOUS STRESS TENSOR
μ	ABSOLUTE VISCOSITY
ν	STOICHIOMETRIC COEFFICIENT

SYMBOL	LIST OF SUBSCRIPTS
i	COORDINATE DIRECTION OR i^{th} SPECIE
n	DERIVATIVE WITH RESPECT TO n
o	FREE STREAM
p	PRODUCTION REGION
s	DERIVATIVE WITH RESPECT TO s
T	TRANSFER REGION

LIST OF SUPERSCRIPTS

$\sim$	FARRE AVERAGED
$-$	TIME AVERAGE

1.0 RESEARCH OBJECTIVES AND SUMMARY

The work described in this report represents the results of research conducted on turbulent reacting flows in air-breathing propulsion systems. The effort involves an assessment of research on supersonic combustion and the preparation of a modular model for delivery to the Air Force at Wright-Patterson Air Force Base. The specific objectives of this research are summarized as follows:

a) SUPERSONIC COMBUSTION

Objective: Under this task area an assessment of supersonic combustion research was to be carried out. The emphasis of this effort involves the identification of fundamental phenomena that require research in order to improve our understanding of fuel injection, mixing, flame stabilization and flame propagation in supersonic combustion ramjet engines.

Research Results: The results of the research conducted on this task include the identification of pressure-turbulence interactions as a potential explanation for trends in turbulent transport and mixing rates observed in supersonic flows. An approach to the modeling of these interactions including direct coupling of the turbulence levels to pressure gradient and pressure fluctuations is outlined in this report.

b) MODULAR MODEL

Objective: Under this task a model applicable to the analysis of two and three dimensional combustion processes is to be prepared for the Air Force (AFWAL/PORT) at Wright-Patterson Air Force Base. A computer code and associated documentation is to be delivered to the Air Force.

Research Result: A basic modular model computer code was prepared and delivered, together with documentation, to the Air Force at Wright-Patterson Air Force Base. This modular model is designed for parametric studies of the efforts of operating conditions and geometric factors on flame stabilization and combustion efficiency. It is specifically relevant to the determination of chemical kinetic limitations on the combustion processes in flow regions typically found in sudden expansion burner configurations such as integral rocket ramjet and ducted rocket combustion chambers. This work

is separately documented in a report entitled "A Simple Reactor Flow Computer Code for the Analysis of Kinetic Efforts in Sudden Expansion Dump Combustors", Report No. SAIC

2.0 INTRODUCTION

The advent of large scale space operations and interest in wide area defense measures have revived interest in hypersonic propulsion systems using airbreathing, supersonic combustion ramjet engines.

Supersonic combustion has been studied for a number of years, with much of the prior emphasis having been on the demonstration that a supersonic fuel-air mixture could be ignited and burned under some conditions. There has been far less emphasis on understanding some of the more fundamental physical problems that accompany supersonic combustion processes. Chemical kinetics and mixing have been observed to be limiting mechanisms in high speed flows and have been responsible for flame stabilization and poor combustion problems even when hydrogen is the fuel. These problems become more critical when storable fuels such as liquid hydrocarbons and slurries are used because of the additional times required for spray evolution, mixing and reaction of the less reactive gaseous and particulate components of these fuels. Thus, the problem is extremely complex because of the involvement of a number of interacting mechanisms. However, common to the supersonic combustion process and independent of the fuel is the pressure field that is developed due to mixing, as well as geometry, and the interaction of the instantaneous pressure field with the turbulence in the flow. Chief among the phenomena that are not well understood in supersonic flow is the unexplained rate of mixing which may be due, at least in part, directly to pressure gradient and pressure fluctuation effects. It has been evident for some years that supersonic shear layer mixing rates are different from those encountered in shear layers at lower speeds, and indeed, different from the mixing rate observed in a low-speed, two-fluid mixing layer in which the density ratio is the same as that observed across a supersonic shear layer. Since shear layers and the attendant mixing phenomena are encountered in a variety of forms throughout the flowfield found within a supersonic-combustion ramjet (scramjet) combustion chamber, this unexplained mixing rate phenomenon is of critical importance in understanding the ignition and combustion process in supersonic flows.

Because the physical cause of the difference in mixing rate between a subsonic variable-density (two-fluid) mixing layer and a supersonic mixing layer having the same overall density ratio is not well understood, attempts to describe this phenomenon have rested primarily on the development of empirical factors which are intended to characterize the modification of the turbulent kinetic energy distribution in supersonic flows compared to that which exists in an "equivalent" subsonic flow. But since these factors are not founded on basic grounds, it is not surprising that the application of them fails to predict observations which have been made in supersonic flows of current interest. For the same reason, little confidence in the applicability of these semi-empirical factors over a broad range of conditions can be expressed. Thus what is required is the development of more fundamental physical descriptions of the phenomena that affect the mixing rate in supersonic reacting flows. Such a development will reduce the high level of uncertainty that now attends estimates of mixing and combustion rates in a scramjet engine.

3.0 RESEARCH STATUS

There is considerable evidence that a major reason for the lack of understanding in supersonic mixing is a lack of knowledge regarding the effects of both mean and fluctuating pressure gradients on the mixing rate in a compressible flow. These effects are apparent in supersonic flames and indeed in subsonic flows, since for all but incompressible flow the contribution to the overall turbulent kinetic energy level of the pressure-related terms can be of the same order of magnitude as all other contributions. Overall, it has been found that the pressure fluctuation and mean pressure gradient effects can manifest themselves as either a source or a sink of turbulent kinetic energy. Thus their effects on the overall mixing rate can be either positive or negative, pointing to a potential for exercising some control of the overall mixing rate in a supersonic flow through control of pressure fluctuations and mean pressure gradients.

In the original development of the turbulent kinetic energy approach to the analysis of turbulent mixing phenomena, attention was restricted to low speed, incompressible and non-reacting flows. In this circumstance the effect of mean pressure gradients with respect to turbulence production is, in terms of the turbulent kinetic energy, identically zero. In an incompressible flow, the effect

of a mean pressure gradient is to redistribute the fluctuating energy among the different components of the turbulence intensity, without affecting the overall energy balance. A fluctuating pressure-velocity correlation remains to be dealt with, but since this has the effect of an additional diffusion term, which is, in many cases of incompressible flow, small compared to the other contributions to the turbulent diffusion of turbulent kinetic energy, this correlation has often been neglected. Despite these rather fundamental limitations with respect to the application of the turbulent kinetic energy equation to more complex compressible and reacting flows, analyses of these more complex phenomena have been made, often with unexplained good success. However, in some fundamental and technologically relevant circumstances the analysis of flow phenomena using the incompressible turbulent kinetic energy approach has not been successful. The supersonic planar shear layer provides a case in point.

A considerable amount of data, collected and analysed for use in the 1972 NASA-Langley conference on free turbulent shear flows, involved the planar free shear configuration. These data, reviewed by Birch and Eggers (Ref.1), involved determinations of the spread rate parameter, σ, in low speed, single-gas, compressible, single-gas, and low-speed, two-gas flows. This spread rate parameter is a measure of the width of the shear layer, and is easily obtained from experimental velocity profiles, or from simple visual observations. Although σ is a parameter that arises from the analytical solution for a fully self-similar two-dimensional flow, a specific definition can be expressed by the equation

$$\sigma = C1 * (X2 - X1) / (Y2 - Y1) \qquad (1)$$

where Y2 and Y1 are the shear layer widths at X2 and X1, respectively. The constant C1 depends on the width definition. If the shear layer width, for example, is defined as that between (U - U1)/(U2 - U1) = 0.10 and (U - U1)/(U2 - U1) = 0.90, where U1 and U2 are the velocities on the different sides of the shear layer, then C1 = 1.855 (Ref.2). Note that as σ increases, the rate of growth of the shear layer decreases.

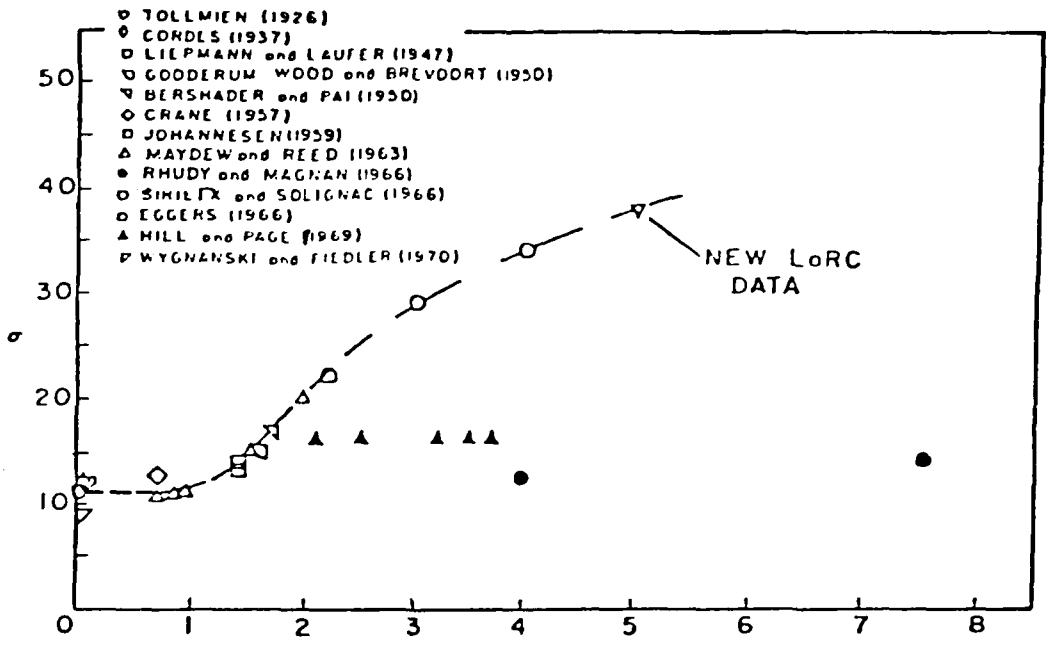

Figure 1. Variation of σ with mach number.

Birch and Eggers (Ref. 1) found that the available data for supersonic shear layer growth rates fell into two distinct groups, as can be seen from Fig. 1. One group of data indicates a sharp increase in σ as the Mach number increases, while the other group, represented here by the data of Hill and Page (but not, in fact, limited to just these data alone) shows an initial rise in σ as Mach number increases, but then a leveling off of the increase. Birch and Eggers suggest that the results which indicate a rapid rise in the spread rate parameter with Mach number are the more accurate, since the results of Hill and Page are in a developing, rather than a fully-developed shear layer. However, the length-based Reynolds number for these data is quite similar to that of the other results shown. An alternate hypothesis for the difference in these results, discussed by Harsha (Ref. 3) notes that the shear layer width measured by Hill and Page was as large as 2.4 inches in a 4 inch x 4 inch wind tunnel, for the Mach 3.5 condition. This would introduce both effects of three-dimensionality and of pressure gradients.

The rapid rise in shear layer growth rate encountered in the supersonic shear layer is not observed in the "equivalent" subsonic shear layer. The equivalency referred to involves the density ratio between the two streams. For example, if two air streams at the same total temperature are considered, one at M = 2 and the other at M = 0.5, a planar mixing layer between the streams will have a density ratio of 1.7 across it. A similar density ratio can be obtained in a subsonic flow through the mixing of dissimilar gases. For example, the mixing of streams of methane and air would provide an equivalent density ratio. But cold-flow mixing of methane and air, as in this example, would not result in the same shear layer growth rate, at the same velocity and density ratio, as results in the supersonic case. In fact, Brown and Roshko (Ref. 4) found that a velocity ratio of 0.377, density ratios of up to a factor of 49 resulted in only a 60% change in σ .

These observations have a considerable import with respect to the use of Morkovin's hypothesis in the application of turbulence models to compressible flowfield prediction. As outlined by Bradshaw (Ref. 5), Morkovin's hypothesis involves the argument that as long as pressure fluctuations are small compared to the mean pressure, and total temperature fluctuations are small compared to the mean total temperature, then

$$\rho'/\bar{\rho} \simeq - T'/\bar{T} \simeq (\gamma - 1)\, M^2 u'/\bar{U}$$

and this quantity will be small as long as $u' / \bar{U}$ is small and $(\gamma - 1)\, M^2$ is not large compared to unity. If the fluctuation in density is sufficiently small then it can be neglected from the standpoint of turbulent transport. Under these conditions a description of the turbulent transport process based on incompressible flow is adequate. This hypothesis has been successfully used in the study of the development of compressible turbulent boundary layers. Clearly it fails for turbulent shear layers, and because of the difference between supersonic shear layers and the "equivalent" variable-density flow, this failure is a result of flow compressibility alone.

The observation of compressibility effects in supersonic shear layer development led to the investigation of several "compressibility correction" techniques intended to modify the turbulent kinetic energy distribution in supersonic flow compared to that which exists in subsonic flows. One such approach is that described by Oh (Ref. 6). Oh's approach focused on the pressure-velocity correlation term normally included in the overall diffusion of turbulent kinetic energy, and specifically on a correlation between the fluctuating pressure and velocity dilatation. The development of the model involves invoking the existence of eddy Mach waves which, following Phillips (Ref. 7) are supposed to be generated whenever the difference in velocity between the high-speed side of a shear layer and the covection velocity of an eddy exceeds the speed of sound in the high-speed fluid. This model is sketched in Fig. 2, and requires that lateral transport of eddies take place rapidly enough that they retain much of their longitudinal velocity as they traverse the shear layer. Based on this model, and using the continuity equation to write the pressure-dilatation correlation in terms of mean flow quantities, Oh arrives at the expression given by Eq. 2:

$$M > 1: \quad \frac{p' \partial u_i}{\partial x_i} = - \frac{c\sqrt{\bar{M}^2 - 1}\, q}{\bar{M}} \left(\bar{\rho} \frac{\partial \bar{U}_i}{\partial x_i} + \text{sign} \left\{ \frac{\partial M}{\partial y} \right\} (\bar{U}_1 - \bar{U}_2) \frac{\sqrt{\bar{M}^2 - 1}}{\bar{M}} \frac{\partial \bar{\rho}}{\partial y} \right)$$

$$M < 1 \quad \frac{p' \partial u_i}{\partial x_i} = 0 \qquad (2)$$

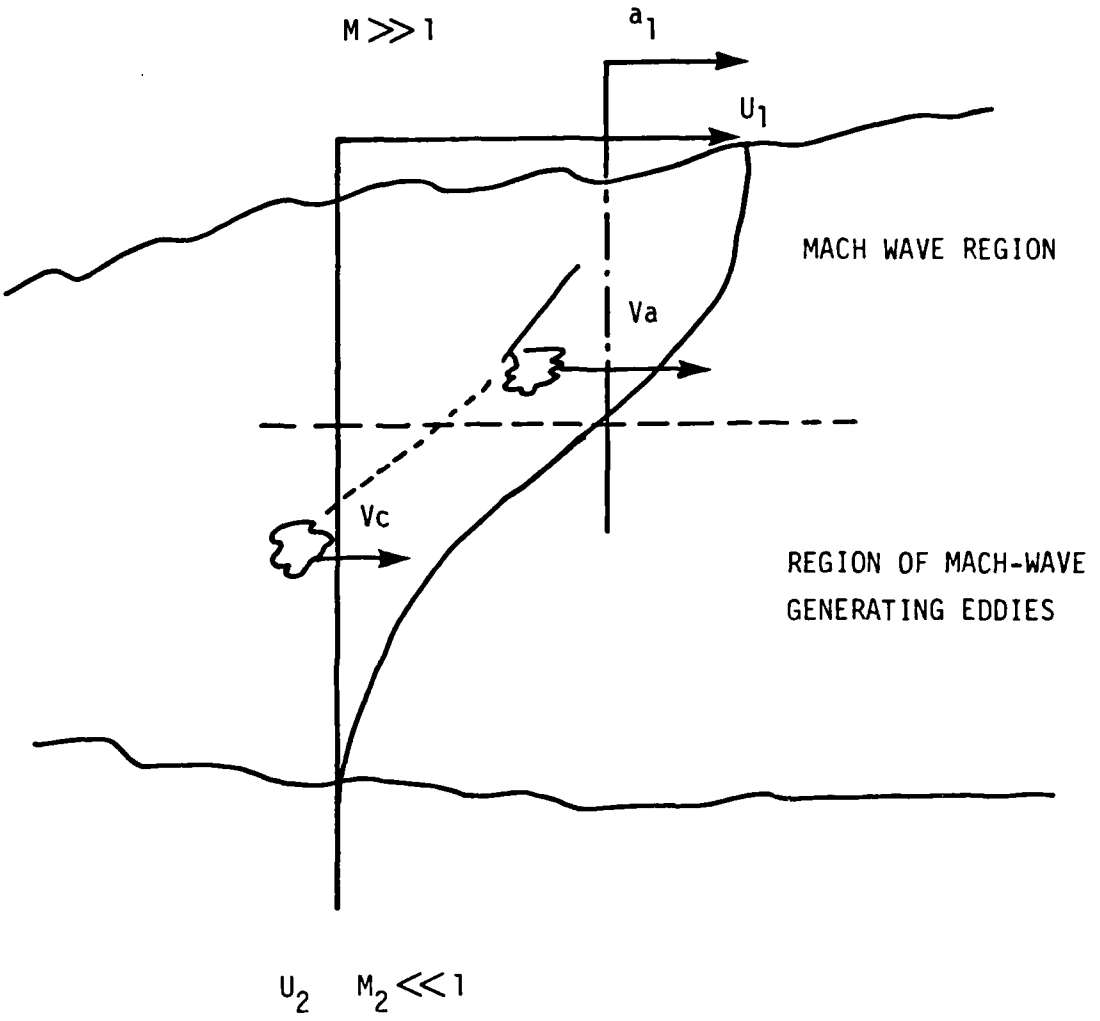

Figure 2. Schematic of Eddy Mach Wave Generation Mechanism.

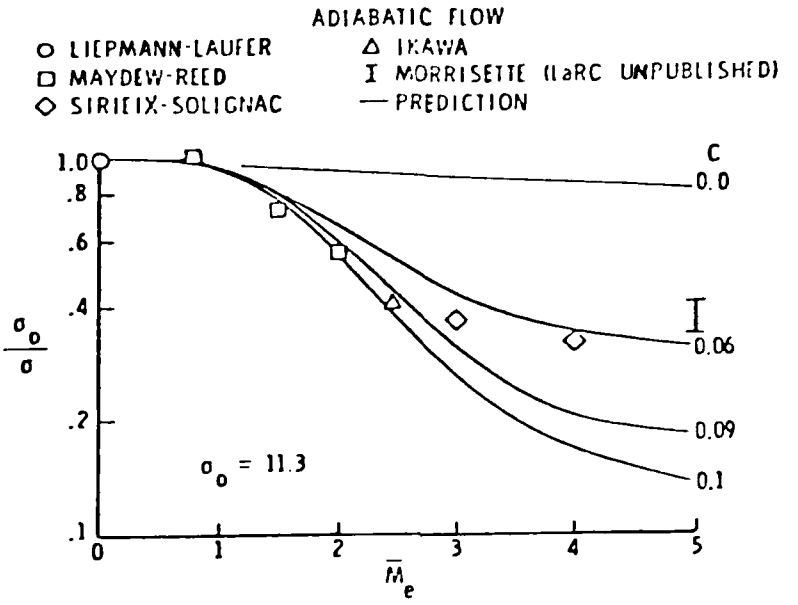

Figure 3. Effect of Mach Number on Predicted Spread Rate of a 2-D Shear Layer, Based on OH's Correlation.

This semi-empirical approach provides the desired result for the spread rate of a supersonic shear layer, as shown by the results presented in Fig. 3; the restriction applied to the use of the correction for $M < 1$ enables the subsonic variable-density results to be recovered as well. However, no direction is provided by this approach with respect to the treatment of the supersonic, two-fluid shear layer, which is a fundamental flow element in a scramjet flowfield.

Dussage, et al. (Ref. 8) consider in some detail the properties and role of the production of turbulent kinetic energy in a non-reacting supersonic flow. In their analysis, the turbulent kinetic energy production term is separated into three parts, one representing production due to pure strain, without density change, another to pure dilatation effects, and a third which expresses the explicit effects of mean pressure-gradients. These three components are given by Eqs (3)-(5) below, using mass-averaged (Favre-averaged) variables*:

Pure Strain

$$P_{IV} = -\left(\overline{\rho u_i'' u_j''} - \frac{1}{3}\,\overline{\rho u_k'' u_k''}\,\delta_{ij}\right)\left[\frac{1}{2}\left(\frac{\partial \tilde{U}_i}{\partial x_j} + \frac{\partial \tilde{U}_j}{\partial x_i}\right) - \frac{1}{3}\,\frac{\partial \tilde{U}_k}{\partial x_k}\,\delta_{ij}\right] \qquad (3)$$

---

* Favre-averaging has been considered to provide a more natural set of dependent variables in a compressible flow. They can be defined by the relation

$$\bar{\rho}\,\underset{\rightarrow}{\tilde{g}} = \frac{1}{t_0}\int_0^{t_0} \rho \underset{\rightarrow}{g}(t)\, dt$$

whereas the conventional (or Reynolds - average) variable can be defined as

$$\underset{\rightarrow}{\bar{g}} = \frac{1}{t_0}\int_0^{t_0} \underset{\rightarrow}{g}(t)\, dt$$

where $\underset{\rightarrow}{g}$ is any vector quantity characterizing the flow.

Pure Dilatation

$$P_V = \frac{1}{3}\,\overline{\rho u_k'' u_k''}\,\frac{1}{\bar{\rho}}\,\frac{D\bar{\rho}}{Dt} \qquad (4)$$

Pressure Effects

$$P_p = -\,\overline{u_i'\,\frac{\partial P}{\partial x_i}} + \overline{(\rho' u_i''/\bar{\rho})}\,\frac{\partial \bar{P}}{\partial x_i} - u_i'\,\overline{\frac{\partial p'}{\partial x_i}} \qquad (5)$$

Note that the fluctuating velocity-pressure gradient correlation term in Eq. 5 is neglected in the rest of the analysis described by Dussauge, et al. Using an order-of-magnitude analysis technique, Dussauge, et al. consider the influence of the different production terms for a supersonic compression and a supersonic expansion. The results indicate that the mean pressure gradient production mechanism enters in the expanding flow (a shear layer downstream of a backstep), where the dilatation effect is also of the same order of magnitude. In the case of the compression, the isovolumetric production term dominates the overall production of turbulent kinetic energy, and indeed essentially reduces to the "incompressible" form. Dussauge, et al. also consider eddy lifetimes in relation to average flow times, and find that for the supersonic expansion, the eddy lifetime is long compared to the flow time through the expansion process. This, they argue, indicates that in this case the changes in turbulence pattern that are observed must come from the production of turbulent kinetic energy and is not as a result of alterations in the turbulent kinetic energy dissipation rate, which would take longer to manifest themselves. The relationship is reversed in the compression case examined. From the standpoint of its relevance to a supersonic-combustion ramjet flowfield, this analysis indicates that different effects of mean pressure gradient should be expected to be manifest in different parts of the combustor flow.

Substantial effects of pressure gradients and pressure fluctuations have also been predicted to occur in low speed flames. For example, Libby and Bray (Ref. 9) show that in a low-speed flame the action of the mean pressure gradient or density inhomogeneities produces countergradient diffusion. The Rankine-Hugoniot relations show that the fluid experiences a small decrease in pressure upon traversing a

flame zone. Burned gas pockets, being of lower density than unburned gas pockets, will respond more readily to this decrease, and will exhibit a tendency to be driven farther downstream than the unburned gas. This effect on turbulent transport can be dominant (and is in a countergradient direction) if the heat release is large compared to the initial thermal enthalpy, even though the effect of the pressure gradient on the average flux of momentum is entirely negligible.

While Libby and Bray focus attention on the effect of mean pressure gradient and neglect all effects of pressure fluctuations, Strahle and Chandra (Ref. 10) neglect all effects of mean pressure gradient and focus attention on the effects of pressure fluctuations, again for a low-speed flame. This focus demands the development of modeling of the pressure-velocity correlation term appearing in the turbulent kinetic energy balance equation. In Favre-averaged variables, Strahle and Chandra write the turbulent kinetic energy equation in the form:

$$\bar{\rho}\,\tilde{U}_i\,\frac{\partial\tilde{q}}{\partial x_i} = -\,\overline{\bar{\rho}u_j''u_j''}\,\frac{\partial\tilde{U}_i}{\partial x_j} - \frac{\partial}{\partial x_i}\,\overline{(\bar{\rho}u_i''q'')} - \Phi - \overline{\frac{u_i''}{\gamma M_0^2}\,\frac{\partial p'}{\partial x_i}} \qquad (6)$$

and consider in detail the modeling of the last term on the right-hand side of Eq. (6). In equation (6) all of the variables are in a non-dimensional form which is itself based on the use of high activation energy asymptotics to define the structure of the premixed flame being considered. The term Φ represents the dissipation of turbulent kinetic energy and is neglected in the further development of the modeling in Ref. 10. Strahle and Chandra proceed by dividing the velocity field into vortical and dilatational components, since, loosely, vortical fluctuations can be identified with turbulence generation and dilatational fluctuations with acoustic motions. By carrying out a detailed order-of-magnitude analysis, they find that at high heat release rates the pressure fluctuations are primarily dilatational and hence do not strongly affect the turbulence energy balance. At lower rates of heat release, the primary mode of fluctuation involves the vortical components, and it is under these circumstances that a model for the pressure-velocity fluctuation term in Eq (6) is required. For a planar, one-dimensional premixed flame, and under the somewhat disturbing but nevertheless necessary assumption that Favre- and Reynolds-averaged variables can be equated, there results the expression:

$$\frac{u'\cdot\nabla p'}{\gamma M_0^2} = \alpha\bar{\rho}\,\frac{d\bar{q}}{dx}\,\frac{d^2\tilde{W}}{dx^2} \qquad (7)$$

where α is a constant of order unity and W represents the dilatational component of the total velocity vector. Because Eq (7) involves the second derivative of the dilatational component it is clear that dilatation is required for the correlation to exist. Heat release is necessary.

By using Eq (7) in a suitably modified form of the Bray-Libby theory (Ref. 9) Strahle and Chandra show that, depending on the magnitude chosen for α, substantial effects on the turbulent kinetic energy balance can be predicted to arise from the pressure fluctuations in a model reacting flow. In general, Eq. 7 represents a source of turbulent kinetic energy and acts to increase the turbulent flame speed. Taken together, what both the analysis of mean pressure gradient effects of Ref. 9 and of pressure gradient fluctuations in Ref. 10 show is that neglecting either of these terms in a general reacting flow problem can be an erroneous assumption. However, both of these analyses are limited to a simple one-dimensional premixed, fast chemistry, flame approximation, and a great deal of work remains to be done to generalize these results to conditions of interest in the analysis of supersonic reacting flow.

An important factor in a theoretical approach is the role played by the turbulent length scale. Representing a mean eddy size, this length scale enters the definition of the turbulent kinetic energy dissipation rate, and has been utilized as well in the definition of modeling for the fluctuating pressure-strain correlation terms (e.g., Rotta, Ref. 13). However, in all turbulent shear flows, a spectrum of eddy sizes and therefore length scales exists, and thus the use of a single length scale is equivalent to an assumption that all length scales are proportional, so that any one can be used to characterize the flow - an "equilibrium" assumption. Our hypothesis is that in the presence of strong pressure gradients and compressibility effects this "equilibrium" no longer exists, so that different length scales need to be defined for turbulence dissipation and for the pressure-strain interaction, for example.

One piece of evidence for this hypothesis is the work reported by Hanjalic', et al. (Ref. 14) involving the passage of a grid-generated decaying turbulent flow through a contraction section. During this process, the kinetic energy is observed to increase and then decay again, but at a slower rate than before. Two-equation

model predictions either underpredict the secondary energy peak and the subsequent rate of decay, or overpredict both, depending on the constants selected. A model incorporating two scales does successfully predict this flowfield, and the results show that as the flow proceeds through the contraction section (and thus through a mean pressure gradient), the initially equilibrium relationship between the two scales of motion is altered.

An investigation was carried out of the multiple-dissipation-length scale approach (Fabris, Harsha, and Edelman) Ref. 15 and it found that even in relatively simple flows it provides a greater generality than the basic two-equation model: round jet predictions can be made with the same coefficients as for other simple flows, for example. However, this work did not involve consideration of the pressure-strain term, or of strong pressure gradients, or of compressible flow, all of which are of potential importance in high speed flows.

Viewed from the perspective of a multiple length scale model, the existence of coherent structures represents the behavior of the flow at the largest scales of interest. Energy is transferred from these scales to the smaller scales of motion, and it is this transfer process that provides the connection between the observed coherent structure and classical turbulent flow models. Previous work (Hanjalic', et al. Ref. 14 , Fabris, et al, Ref. 15) has limited the number of scales to be considered, the transfer mechanism which we believe is Reynolds number dependent and the equation formulation. Thus, in the previous work the Reynolds averaged variables have been used, with two scales and a direct transfer of energy independent of local flow Reynolds number. For the flows to be considered in this work, the approach is to systematically increase the number of scales considered, with the largest scale described as a periodic (or quasi-periodic) fluctuation, and a local Reynolds number-related energy transfer rate. At the other end of the spectrum, a small-scale energy dissipation rate can be defined to represent mixing on a scale consistent with that which applies to chemical reactions.

In contrast, both the algebraic Reynolds stress model (ASM) and the k-ϵ approaches are single-point models which adopt a single time scale proportional to the turbulence energy turnover time, k/ϵ . However, it is overly simplistic, at least conceptually, to assume that a single time scale can successfully characterize the rates of progress of different turbulent interactions.

The key to the new multiple-scale approach is the recognition that while the dissipation equation and the kinetic energy equation both contain production and dissipation terms, these processes occur in different spectral regions of the flow. That is, turbulence energy production occurs in the larger eddies in the flow, while dissipation phenomena involve primarily the smaller scales. Thus, there must be a transfer of energy from the larger scales to the smaller, and this transfer can, in certain situations, introduce a lag phenomenon, so that turbulence energy production and turbulence dissipation do not necessarily both increase or decrease in the same region of the flow as is implied by a single-scale model.

To introduce a model in which the evolution of the different scales appropriate to the large-eddy production region and the small-eddy dissipation region can be accounted for, we introduce a partitioning of the turbulence energy and its dissipation rate into three regions. For wave numbers less than κ_1, a production region is defined, characterized by a turbulent kinetic energy k_p and a dissipation rate ϵ_p. This dissipation rate controls the transfer of energy through the transfer region $\kappa_1 < \kappa < \kappa_2$. For wave numbers higher than κ_2, turbulence energy is dissipated as heat. A separate kinetic energy and dissipation rate equation is written for the transfer region, characterized by k_T and ϵ_T, and the production term in the kinetic energy equation for the transfer region is equal to the dissipation rate ϵ_p in the production region.

The partitioning of the energy spectrum into three regions, as in this example requires two sets of transport equations, given the assumption (basic to most turbulence modeling) that the mechanisms involved in the final dissipation of turbulent kinetic energy into thermal energy are capable of accepting all of the energy transferred to them. This assumption is the reason that the physical fluid viscosity does not appear in the turbulence dissipation rate equations.

The model equations for the production and transfer region turbulent kinetic energy and dissipation rate are similar in form to the standard k and ϵ transport equations. They can be written as follows:

Production Region

$$\frac{\partial k_p}{\partial t} + U_k \frac{\partial k_p}{\partial x_k} = P_k - \epsilon_p + \frac{\partial}{\partial x_k}\left(\left(\nu + \frac{\nu_t}{\sigma_k}\right)\frac{\partial k_p}{\partial x_k}\right) \tag{8}$$

$$\frac{\partial \epsilon_p}{\partial t} + U_k \frac{\partial \epsilon_p}{\partial x_k} = c_{p_1} P_k \frac{\epsilon_p}{k_p} - c_{p_2} \frac{\epsilon_p^2}{k_p} + \frac{\partial}{\partial x_k}\left[\left(\nu + \frac{\nu_t}{\sigma_\epsilon}\right)\frac{\partial \epsilon_p}{\partial x_k}\right] \tag{9}$$

Transfer Region

$$\frac{\partial k_T}{\partial t} + U_k \frac{\partial k_T}{\partial x_k} = \epsilon_p - \epsilon_T + \frac{\partial}{\partial x_k}\left[\left(\nu + \frac{\nu_t}{\sigma_k}\right)\frac{\partial k_T}{\partial x_k}\right] \tag{10}$$

$$\frac{\partial \epsilon_T}{\partial t} + U_k \frac{\partial \epsilon_T}{\partial x_k} = c_{T_1} \frac{\epsilon_p \epsilon_T}{k_T} - c_{T_2} \frac{\epsilon_T^2}{k_T} + \frac{\partial}{\partial x_k}\left[\left(\nu + \frac{\nu_t}{\sigma_\epsilon}\frac{\partial \epsilon_T}{\partial x_k}\right]\right. \tag{11}$$

in which the subscript p refers to the production region and T to the transfer region. In this formulation, the turbulent viscosity is given by

$$\mu_T = \rho c_\mu \left(k_p + k_T \right) \frac{k_p}{\epsilon p} \tag{12}$$

and

$$\rho_T = -\overline{u_i u_j} \quad \frac{\partial U_i}{\partial x_j} \tag{13}$$

In this example, the equations are written in incompressible Reynolds-averaged form. For a compressible flow, these equations can be derived either in Reynolds-averaged or Favre-averaged form. If they are derived in Reynolds-averaged variables, correlations which involve density fluctuations are introduced, and these turbulence correlation expressions take a different form if Favre-averaged variables are used. The choice of which form of equations to use in the theoretical analysis is dependent on the instrumentation and measurements involved in the experimental program: laser diagnostics, for example, measure the time-average fluctuations which can be used to construct the Reynolds-average correlations, providing a means for obtaining density fluctuations and their correlations (as well as pressure fluctuations) is available. In addition, the equations have been written in time-dependent form to account for large-scale, quasi-periodic motions of coherent structures.

Note also that in writing equations 8-11 the pressure fluctuation terms have been neglected, but their inclusion is straight forward. Also, equations 8-11 indicate a two-scale breakdown in which the production of transfer region kinetic energy is directly the dissipation of production region kinetic energy. In actuality, there are many more steps to the energy cascade process. For example, energy spectrum observations indicate that the wave number range over which significant energy is contained in the turbulence is considerably wider in the interior region of the flow than on the edges, suggesting, at the outer edge of the flow which is dominated by the large eddies, a more direct transfer of kinetic energy from the large scales to the dissipating scales than is the case in the flowfield interior. Since it is also observed that the large structure is more evident at low Reynolds numbers than at higher Reynolds numbers in jet and shear layer flows, it is also clear that the energy transfer mechanism is Reynolds-number dependent.

In order to gain insight on the magnitude and coupling of the pressure field in supersonic ducted flow a baseline analysis of a simple supersonic combustor flow field has been carried out.

Common to the variety of engines used for hypersonic flight, such as rocket engines, airbreathing engines and composite engines (combinations of both) are the problems associated with propellant combustion. With the exception of the pure solid rocket, the combustion process is coupled to a fuel/oxidizer mixing process. If a spectrum of pressures, temperatures and flow velocities are considered, the combustion process may be (1) diffusion controlled, i.e., fuel dependent only

upon the mixing rate; (2) reaction controlled wherein the kinetics of the oxidation process determine the heat release rate; and (3) an intermediate regime wherein the heat release rate depends upon the coupled mixing and kinetic rates.

The diffusion controlled process is desirable in comparison to the reaction controlled situation because the latter involves mixing process followed by the combustion process and could lead to excessively long combustion chambers. In addition, for hypersonic flight involving pure airbreathing and composite engines. shock losses, dissociation losses and heat transfer limitations require that the flow remain supersonic during the combustion process. Analysis of the supersonic combustion process requires consideration of the coupling between the mixing and kinetic processes because flow, mixing and reaction times are generally of equal order of magnitude. Of particular importance in high speed combustion chamber flows is the optimization of the combustion chamber length required to achieve efficient heat release while maintaining reasonable chamber lengths. To achieve an understanding of the relevant parameters and their inter-relationships, it is necessary to analyze the details of the reacting flowfield. A meaningful analysis for such flow configurations requires including turbulent mixing, finite rate combustion and pressure gradients in a model which appropriately accounts for the coupling of these phenomena. It should be noted that the pressure field must be considered in detail because of the sensitivity to pressure of both the chemical kinetics and velocity field. The structure of the pressure field includes the locally induced pressure due to mixing and combustion as well as the pressure impressed on the flow due to the interactions with the confining walls.

A configuration which characterizes the flows considered in this investigation is shown in Fig. 4. Although the complete flowfield can involve a complex internal shock structure the present form of the analysis does not resolve the pressure field in terms of discrete shock structures.

The classical analysis of viscous flow problems involving unequal characteristic length scales in the coordinate directions leads to the boundary-layer formulation. The describing equations are parabolic and the pressure is constant across the

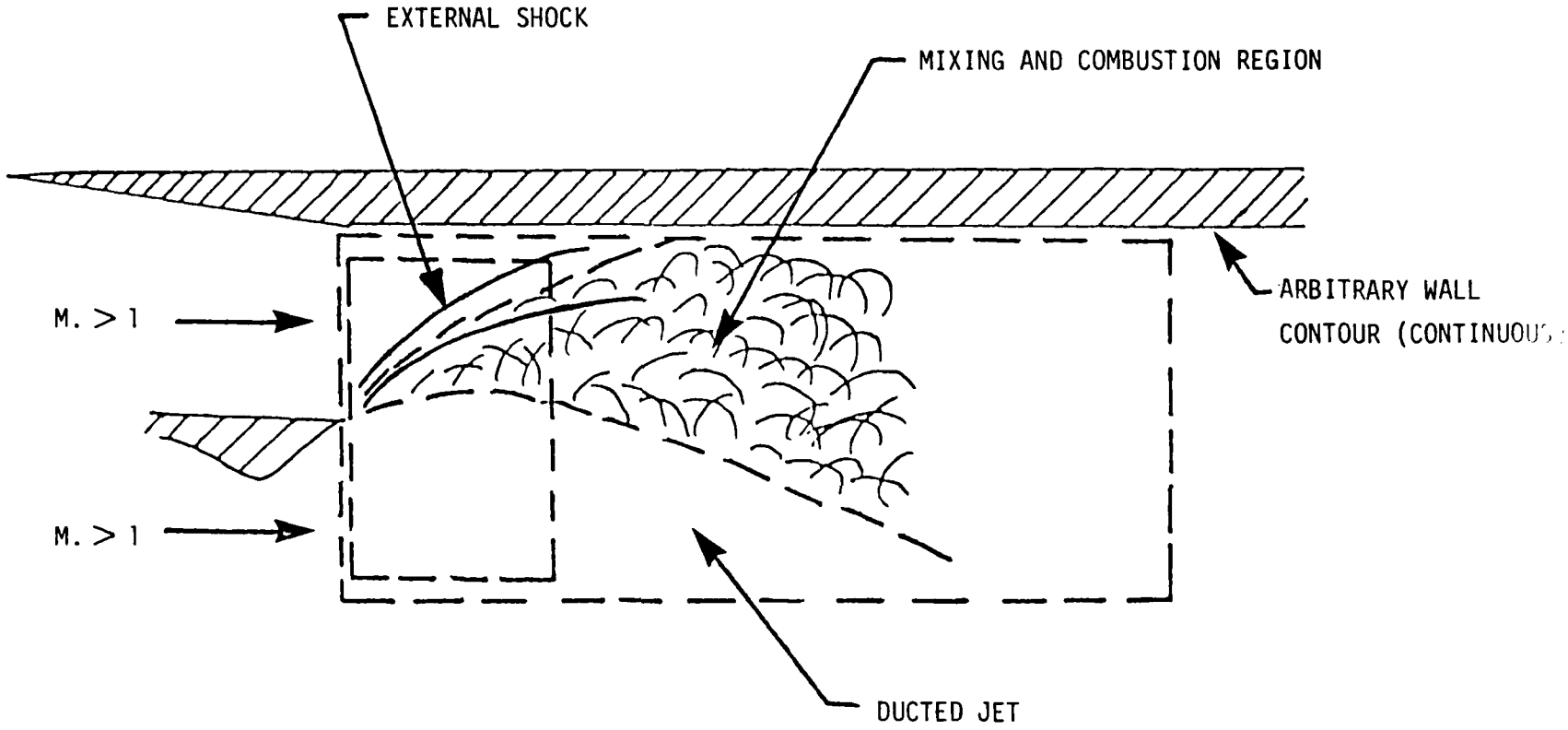

Figure 4. Schematic of Flowfield.

smaller, or lateral, dimension of the flow. The pressure variation in the primary flow direction is either specified as a given distribution or is determined by approximate methods based on the induced pressure due to the displacement of the inviscid outer flow. In either case the pressure across the flow is assumed constant. In flows involving combustion an accurate prediction of the induced pressure field is crucial to predicting the force on solid surfaces adjacent to the combustion region. Moreover, the ignition delay and reaction time of the combustion process itself may be critically dependent on the local pressure, particularly for pressure levels below atmospheric. Furthermore, non-uniform transverse pressure distributions are inherent in jets operating either in an under-expanded or over-expanded configuration. Finally, the coupling of the pressure field to the turbulence levels included in the supersonic flow requires that the pressure field be accurately predicted.

The analysis of this problem requires a study of the full Navier-Stokes equations. The approach involves the choice of coordinates and a set of physically reasonable assumptions which will provide a tractable formulation and yet preserve the basic character of the flow.

The general describing equations for the steady flow of a reacting mixture of perfect gases are given by:

Global Continuity:

$$\nabla \cdot \rho \underline{V} = 0 \tag{14}$$

Species Continuity:

$$\nabla \cdot \rho \alpha_i \underline{V} = \rho \dot{W}_i - \nabla \cdot \underline{j}_i \tag{15}$$

$i \equiv$ ith specie

Where $\underline{j}_i$ is the diffusional mass flux vector:

$$\underline{j}_i = \rho_i (\underline{V}_i - \underline{V})$$

Momentum:

$$\nabla \cdot \rho \, \underline{VV} = - P + \nabla \cdot \underline{\tau} \tag{16}$$

Where $\underline{\tau}$ is the viscous stress tensor.

Energy:

$$\nabla \cdot \rho \underline{V} H = \nabla \cdot (\tau \cdot \underline{V}) - \nabla \cdot \underline{q} - \nabla \cdot \sum_i h_i \underline{j}_i \tag{17}$$

Where $H = \sum_i \alpha_i h_i (T) + \dfrac{\underline{V} \cdot \underline{V}}{2}$ is the stagnation enthalpy, and $\underline{q}$ is the heat conduction vector.

State:

$$\rho = \frac{P}{RT \sum_i \dfrac{\alpha_i}{W_i}} \tag{18}$$

Transport Processes

The transport processes considered in this investigation include viscous stresses, species diffusion and heat conduction. The models used to represent these processes are as follows:

Vicous Stress

$$\tau = 2\mu \, \underline{\epsilon} - 2/3 \, \mu \, \underline{\delta} : \underline{\epsilon} \, \underline{\delta} \tag{19}$$

Where

$$\underline{\epsilon} = 1/2(V\underline{V} + \nabla * \underline{V}) \tag{20}$$

and $\underline{\delta}$ is the unit tensor.

Species Diffusion

The diffusion of each species is assumed to depend only on the gradient of the particular species mass fraction. This assumption requires equal binary diffusion coefficients D_{ij}, for each species so that Fick's law is applicable.

Under this assumption the diffusional mass flux is given by:

$$\underline{j}_i = - \rho D_{ij} \nabla \alpha_i = - \mu \frac{Le}{Pr} \nabla \alpha_i \qquad (21)$$

Heat Conduction

Consistent with the above assumptions the heat conduction may be represented by the Fourier law given by:

$$\underline{q} = - k \nabla T = - \frac{\overline{c_p}}{Pr} \mu \nabla T \qquad (22)$$

where

$$\overline{c_p} = \sum_i \alpha_i c_{p_i}$$

A schematic of the coordinate system adopted in this analysis is shown in Fig. 5. A coordinate system is sought wherein a minimum of physical assumptions are required to simplify the Navier-Stokes equations and within which a numerical solution is most easily formulated and implemented. The implicit coordinate system provides these desired conditions. Some insight into this choice is obtained by considering the important case of an underexpanded (or overexpanded) jet. The initial flow deflection is governed almost entirely by the adjustment of the pressure. The jet flow is separated from the external flow by the "dividing" streamline and the gradients in velocity, concentration and temperature will be greatest in the direction normal to the streamline. Of course, as the flow becomes more parallel to the jet axis this condition is still satisfied. It appears then that in this coordinate system some of the usual boundary-layer assumptions may be applied. Furthermore, it is shown later that a natural consequence of this is a characteristic method of solution which can be implemented with a certain degree of ease.

Edelman et al., Ref. 16 (1968) have made a systematic order of magnitude analysis in the s-n coordinate system (direction along and normal to a streamline) for Eqs. (14) to (22) for both two-dimensional and axisymmetric flows. The problem involves a class of supersonic jet flows having a principal flow direction which are conditions also found in practical configurations including rocket nozzles and supersonic combustion ramjet engine combustion chambers. In a supersonic flow, small deflections can induce a non-uniform pressure field which can have a

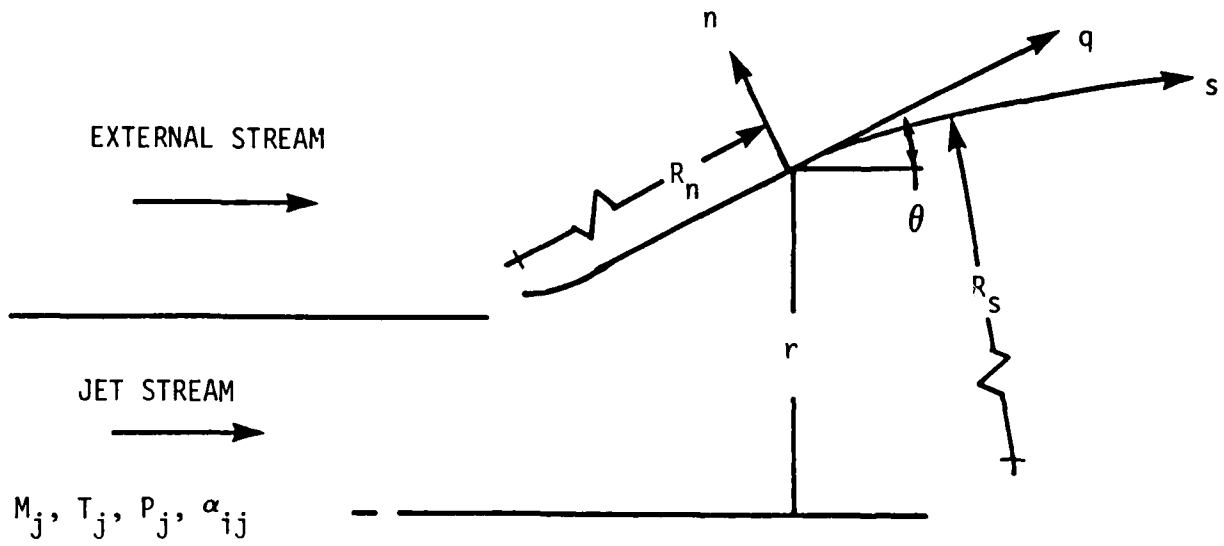

Figure 5. Schematic of Flowfield with Lateral Pressure Gradient.

significant effect upon combustion and pressure forces on surfaces adjacent to the flow. Furthermore, if the flow curvature is small in regions where viscous effects dominate across the entire field, viz., away from the near region of an under-expanded jet, then boundary layer type approximations are applicable to the diffusive terms in the describing equations. They have shown that Eqs. (14) to (22) can be reduced to the following simple form.

Global Continuity:

$$(\rho q)_s + \frac{j \rho q}{r} \sin\theta + (\rho q)_n = 0 \tag{23}$$

s-Momentum:

$$\rho q\,(q)_s + P_s = \frac{1}{r^j}\left[r^j \mu \frac{\partial q}{\partial n}\right]_n \tag{24}$$

n-Momentum:

$$\rho q^2 \theta_s + P_n = 0 \tag{25}$$

Species Continuity:

$$\rho q\,(\alpha_i)_s = \rho \dot{W}_i + \frac{1}{r^j}\left[r^j \mu \frac{Le}{Pr}\,(\alpha_i)_n\right]_n \tag{26}$$

Energy:

$$\rho q\,(H_s) = \frac{1}{r^j}\left[r^j \frac{\mu}{Pr} H_n\right]_n + \frac{1}{r^j}\left[\left(1 - \frac{1}{Pr}\right) \mu\,(q^2/2)_n\right]_n + \frac{1}{r^j}\left[\sum_i (Le-1)\, r^j \frac{\mu}{Pr} h_i\, (\alpha_i)_n\right]_n \tag{27}$$

Where:

$$H = \sum_i \alpha_i h_i (T) + q^2/2 \tag{28}$$

and

$$\rho = \frac{P}{RT \sum_i \frac{\alpha_i}{W_i}} \tag{29}$$

In equations (23) – (29), the subscript notation has been used to indicate partial derivatives, i.e.,

$$(\rho q)_s \equiv \frac{\partial}{\partial s} (\rho q)$$

$$\left[r^j \frac{\mu}{Pr} H_n\right]_n = \frac{\partial}{\partial n}\left[r^j \frac{\mu}{Pr} \frac{\partial H}{\partial n}\right]$$

The solution technique applied to equations 23 through 27 involves the coupling of both hyperbolic and parabolic equations. It is the purpose of the following discussions to describe the details of the method of solution which can be described in terms of an "inner" calculation (characteristics) and an "outer" calculation (mixing).

The characteristics calculation is initiated in a standard manner from a "line" of given data as shown in Fig. 6.

The characteristic directions are dependent only upon the local state and the left (I) and right (II) running characteristic directions from point K, say, are given by:

$$\text{Tan } \epsilon_K = \pm \sqrt{\frac{F}{\rho q^2 \left(\frac{F}{p} - \frac{1}{\rho} - \frac{F}{\rho q^2}\right)}} \tag{30}$$

Where

$$F = T \sum_i \alpha_i \frac{dh_i(T)}{dT} \tag{31}$$

and all properties are evaluated at the point K.

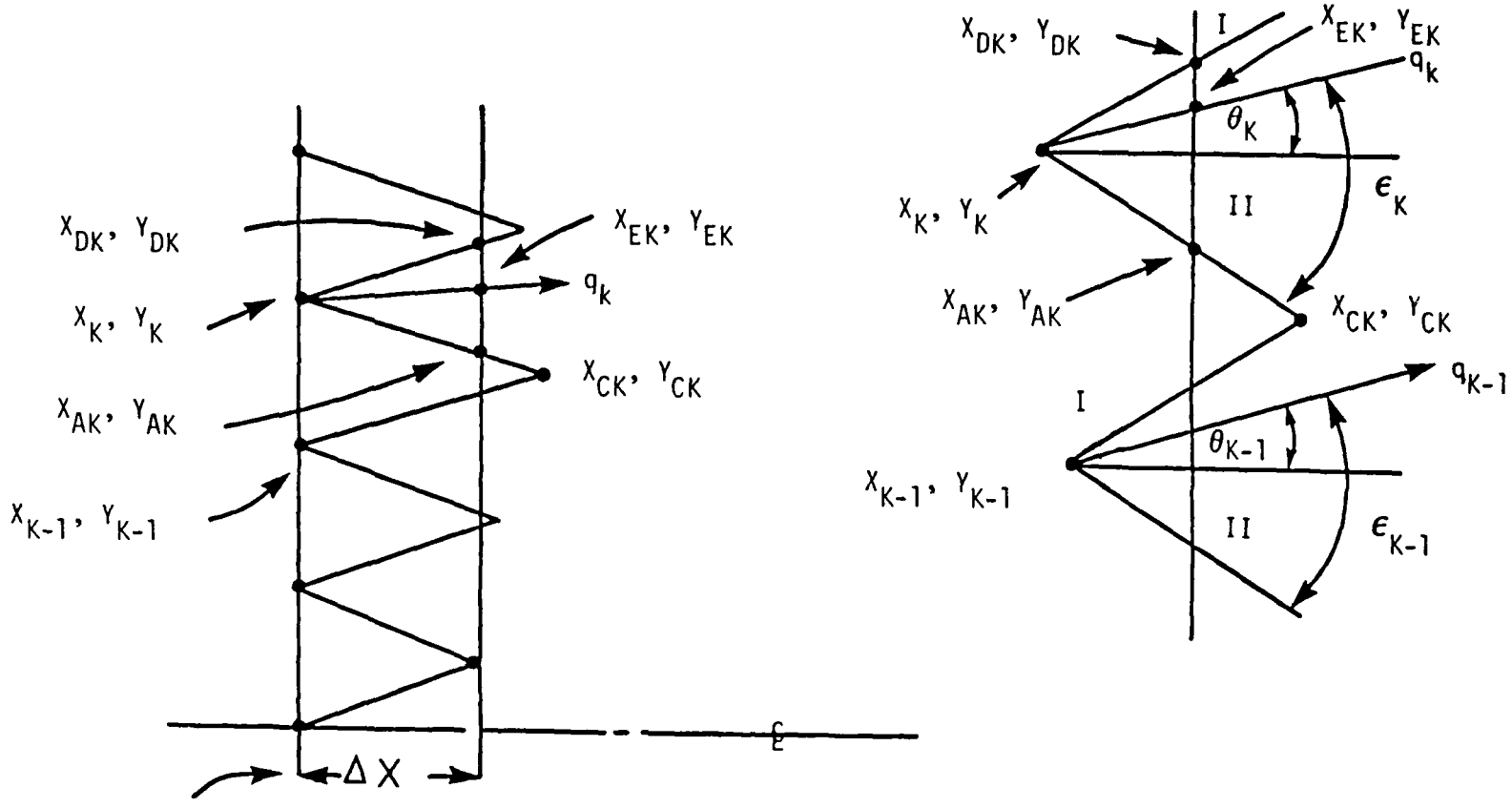

LINE OF GIVEN DATA (DATA IS EQUALLY SPACED AT INITIAL STATION)

Figure 6. Numerical Net for Characteristics Step.

The compatibility equations are obtained in the usual way assuming, however, that the viscous terms are part of the forcing function. These equations provide a relation between the flow deflection ($\theta = \mathrm{Tan}^{-1}\tau$) and the pressure p, and are given by:

$$\frac{d\tau}{d\ell} \pm b \frac{dp}{d\ell} = \pm g \tag{32}$$

Where

$$b = \frac{1 + \tau^2}{\rho q^2 \ \mathrm{Tan}\epsilon} \tag{33}$$

And

$$g = \frac{(1+\tau^2)\sin\epsilon}{F} \left[\frac{\mu}{\rho q} \left(H_{nn} + \frac{\cos\theta}{y} H_n\right) - \frac{\mu}{\rho} \left(1 + \frac{F}{q^2}\right) \left(q_{nn} + \frac{q_n \cos\theta}{y}\right) - \right.$$

$$\left. \sum_i h_i D_i + \frac{\rho RTF}{p} \sum_i \frac{D_i}{W_i} - \frac{F \sin\theta}{y} \right] \tag{34}$$

With

$$D_i = \frac{\mu}{\rho q} \alpha_{inn} + \frac{\mu}{\rho q} \frac{\cos\theta}{y} \alpha_{in} + \frac{\dot{W}_i}{q} \tag{35}$$

The chemical production term, $\dot{W}_i$, represents the production rate of species i through the mechanism of a system of chemical reactions given by:

$$\sum_{j=1}^{N} \nu'_j A_j \underset{k^b_m}{\overset{k^f_m}{\rightleftharpoons}} \sum_{j=1}^{N} \nu''_j A_j \quad , \qquad m = 1, M \ldots \tag{36}$$

where N species are involved in M reactions and the ν_j's are the stoichiometric coefficients associated with A_j species. The production rate, $\dot{W}_i$, is then given by:

$$\dot{W}_i = \frac{\rho}{W_i} \sum_{j=1}^{M} (\nu''_{i,j} - \nu'_{i,j}) \left| k^f_j \prod_{\gamma=1}^{N} y_\gamma^{\nu'_{\gamma,j}} - k^b_j \prod_{\gamma=1}^{N} y_\gamma^{\nu''_{\gamma,j}} \right| \tag{37}$$

Where

$$y_i = \rho \frac{\alpha_i}{W_i} \tag{38}$$

is the molar density of the i^{th} specie.

The sequence of calculations is initiated with a characteristic type calculation. Referring to Fig. 6, the up-running characteristic from point K-1 and the down-running characteristics from point K are constructed and their point of intersection, C_K, is obtained. This procedure is carried out for all intersections across the field. The minimum forward distance required for an intersection determines the "characteristics" step size which guarantees that all new data computed across the field is within the domain of influence of the initial data.

The next step in the sequence of calculations involves the solution of the compatibility equations along the characteristics. The differenced form of Eqs. (32) are given by:

$$\frac{\tau_C - \tau_{K-1}}{\Delta \ell_I} + b_{k-1} \frac{P_C - P_{K-1}}{\Delta \ell_I} = g_{K-1} \tag{39}$$

and,

$$\frac{\tau_C - \tau_K}{\Delta \ell_{II}} - b_K \frac{P_C - P_K}{\Delta \ell_{II}} = -g_K \tag{40}$$

Where

$$\Delta \ell_I = \sqrt{(x_{CK} - x_{K-1})^2 + (y_{CK} - y_{K-1})^2} \tag{41}$$

and,

$$\Delta \ell_{II} = \sqrt{(x_{CK} - x_K)^2 + (y_{CK} - y_K)^2} \tag{42}$$

Solving Eqs. (39) and (40) for the pressure gives:

$$p_C = \frac{\tau_{K-1} - \tau_K + g_{K-1} \Delta \ell_I + g_K \Delta \ell_{II} + b_{K-1} p_{K-1} + b_K p_K}{b_{K-1} + b_K} \tag{43}$$

τ_C is determined by substitution into either Eqs. (39) or (40).

As discussed above, a single forward step size is used and this is done in anticipation of the subsequent mixing calculation discussed below. However, this requires interpolations for the data required at points A, D and finally E (Fig. 6). Thus, the pressure, p, and flow deflection, τ, are determined at A and D by interpolation along the characteristics and then a second interpolation is performed across the field to determine p and τ on the streamline at point E. In this way, the pressure gradient along the streamline is obtained:

$$\frac{dp}{ds} = \frac{p_{EK} - p_K}{\Delta s} \tag{44}$$

This result is utilized in the mixing calculation discussed in the next section.

The explicit bilateral coupling between the pressure field and the viscous mixing process is through the forcing function g in Eqs. (39) and (40) and the momentum equation along the streamline, respectively. The former contains the diffusion and chemical reaction terms and the latter contains the pressure gradient. Furthermore, the description given above for the p-τ determination represents a single calculation in an iterative calculation. Thus, the forcing function is modified by averaging it over a step which includes the "new" diffusion contributions obtained at the end of the mixing calculation. The p-τ calculation is repeated until the difference in two successively determined pressures is less than a prescribed tolerance.

The calculation procedure as described so far lends itself uniquely to the application of already existing numerical solutions of the parabolic mixing problem. The solution is obtained by an explicit finite difference representation of the describing equations along the streamlines. These equations are given by:

Momentum:

$$\rho q \frac{\partial q}{\partial s} + \frac{\partial p}{\partial s} = \mu \frac{\partial^2 q}{\partial n^2} - \left(\frac{\mu \cos\theta}{y} + \frac{\partial \mu}{\partial n} \right) \frac{\partial q}{\partial n} \tag{45}$$

Energy:

$$\rho q \frac{\partial H}{\partial s} = \mu \frac{\partial^2 H}{\partial n^2} + \left(\frac{\mu \cos\theta}{y} + \frac{\partial \mu}{\partial n} \right) \frac{\partial H}{\partial n} \tag{46}$$

Species:

$$\rho q \frac{\partial \alpha_i}{\partial s} = \mu \frac{\partial^2 \alpha_i}{\partial n^2} + \left(\frac{\mu \cos\theta}{y} + \frac{\partial \mu}{\partial n} \right) \frac{\partial \alpha_i}{\partial n} + \rho \dot{W}_i \tag{47}$$

Turbulence:

One-equation TKE model

$$\rho q \frac{\partial e}{\partial s} = \frac{\mu}{\sigma_s} \frac{\partial^2 e}{\partial n^2} + \left(\frac{\mu \cos\theta}{y} + \frac{\partial \mu}{\partial n} \right) \frac{\partial e}{\partial n} + \mu \left(\frac{\partial q}{\partial n} \right)^2 - \frac{a_2 \rho e^{3/2}}{\ell_k} \tag{48}$$

Two-equation TKE model

$$\rho q \frac{\partial e}{\partial s} = \frac{\mu}{\sigma_k} \frac{\partial^2 e}{\partial n^2} + \left(\frac{\mu \cos\theta}{y} + \frac{\partial \mu}{\partial n} \right) \frac{\partial e}{\partial n} + \mu \left(\frac{\partial q}{\partial n} \right)^2 - \rho \epsilon \tag{49}$$

$$\rho q \frac{\partial \epsilon}{\partial s} = \frac{\mu}{\sigma_\epsilon} \frac{\partial^2 \epsilon}{\partial n^2} + \left(\frac{\mu \cos\theta}{y} + \frac{\partial \mu}{\partial n} \right) \frac{\partial \epsilon}{\partial n} + \frac{C_\epsilon \epsilon \mu}{e} \left(\frac{\partial q}{\partial n} \right)^2 - \frac{C_{\epsilon 2} \rho \epsilon^2}{e} \tag{50}$$

It is important to note that the describing equations for mean quantities have been simplified from their most general form by the assumption that the Prandtl and Schmidt numbers are unity. Furthermore, in the numerical representation of the above equations it is assumed that $n \rightarrow y$. Both of these approximations were made to facilitate the initial stages of the program development but it is believed that the limitations are not critical.

To illustrate the numerical solution technique, consider the difference form of Eq. (45) with reference to Fig. 7.

$\sigma \equiv \frac{\text{CHARACTERISTICS}}{\text{STEP SIZE}}$

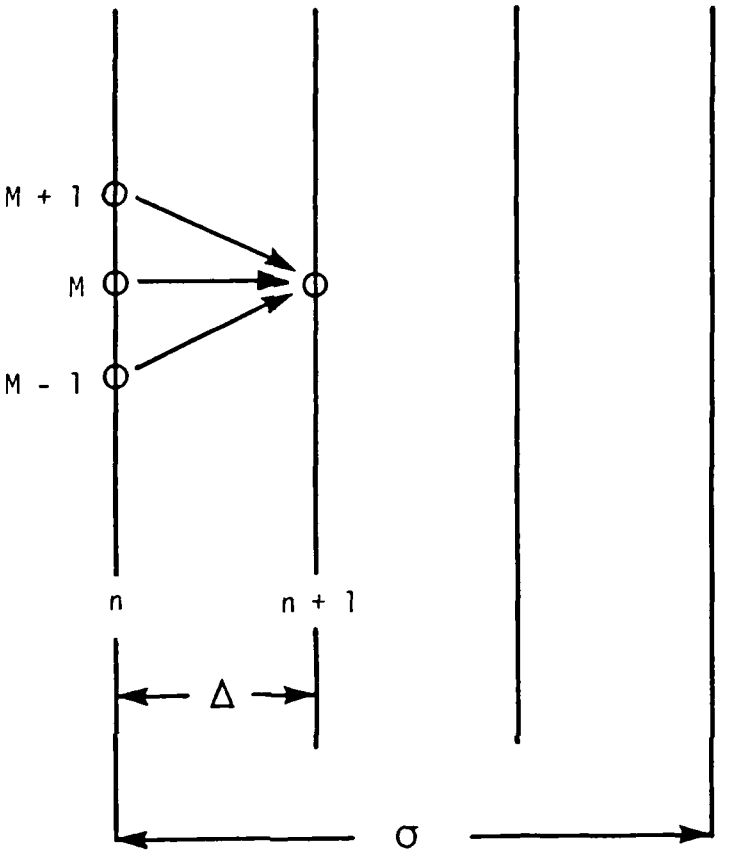

Figure 7. Numerical Grid for Mixing Step.

$$\frac{q_{m,n+1}-q_{m,n}}{\Delta s} = \left(\frac{1}{\rho q}\right)_n \left[\frac{q_{m+1,n}-2q_{m,n}+q_{m-1,n}}{(\Delta y)^2}\ \mu_{m,n}\right.$$

$$\left. + \left\{\frac{\cos\theta_{m,n}\,\mu_{m,n}}{y_m} + \frac{\mu_{m+1,n}-\mu_{m-1,n}}{2\Delta y}\right\}\left(\frac{q_{m+1,n}-q_{m-1,n}}{2\Delta y}\right)\right] - \left(\frac{1}{\rho q}\right)_n \frac{\Delta p}{\sigma} \qquad (51)$$

where $\frac{\Delta p}{\sigma}$ is given by the characteristics calculation (see Eq. (44).

Eq.(51) represents an explicit finite difference form of the s-momentum equation. The energy and species conservation equations assume a similar form. The forward step size is limited by a stability requirement which for linear parabolic equations is given by:

$$\Delta s \leq 1/2\ \ \rho q\ \ \frac{\Delta y^2}{\mu} \qquad (52)$$

To insure stability of the non-linear system a fraction of the characteristic step, σ, is used:

$$\nabla = \frac{\sigma}{\left(\frac{\sigma}{\nabla s} + 1\right) N_s} \qquad (53)$$

where N_s is an input integer. In cases involving fast reacting systems N_s=6 has been found to be sufficient.

The species conservation equation, Eq. (47), is treated in a special way for configurations involving finite rate kinetics. The equations for turbulent kinetic energy e and dissipation rate ϵ are also treated differently to avoid negative values which are unphysical. In the beginning of the calculations when both diffusion and production are negligible, the dissipation term (last terms in Eqs. (48) and (50) when expressed explicitly in the finite difference representation can give negative values for e and ϵ under certain circumstances. This is avoided by partly implicitizing the dissipation term. Thus, $e^{3/2}$ and ϵ^2 in the dissipation term are approximated as $(e_{m,n+1})\ (e_{m,n})^{1/2}$ and $(\epsilon_{m,n+1})\ (\epsilon_{m,n})$ respectively. Thus Eq.

(48) can be approximated as:

$$e_{m,n+1} = e_{m,n} + X_{m,n} \Big/ 1 + \frac{\nabla s \; a_2 \; e_{m,n}^{\frac{1}{2}}}{q_{m,n} \; \ell_k} \qquad (54)$$

where $X_{m,n}$ represents the diffusion and production term.

The above discussions pertain specifically to the solution technique for the describing partial differential equations. To completely specify a given problem the initial and boundary conditions must be given. In the present report a shockless ducted jet flow configuration is described. The wall is assumed to be impermeable, and adiabatic. The boundary conditions are given by:

$$x > 0 \; , \; y = y_w(x) \begin{cases} \left(\dfrac{\partial \alpha_i}{\partial y}\right)_w = 0 \\ \left(\dfrac{\partial H}{\partial y}\right)_w = 0 \\ \dfrac{\partial q}{\partial y} = -\dfrac{c_f}{2} \left(\dfrac{\rho q^2}{\mu}\right)_{mean} \end{cases} \qquad (55)$$

The arbitrary wall contour, $y = y_w(x)$ may be specified in terms of the coefficients of 5^{th} order polynominals covering four adjoining regions:

$$y_w = \sum_0^5 a_n x^n \qquad (56)$$

The pressure is determined from the appropriate uprunning characteristic since the flow deflection at the "new" wall point is known from Eq. (56).

The calculation proceeds as follows (see Fig. 8):

A characteristic step is taken to determine the minimum forward distance, σ, for intersections. A star, *, point is found by interpolation between the w_n and KT_n points whose uprunning characteristic intersects the wall at the end of the step, $x_{n+1} = x_n + \sigma$. The pressure at the wall is then computed through the compatibility

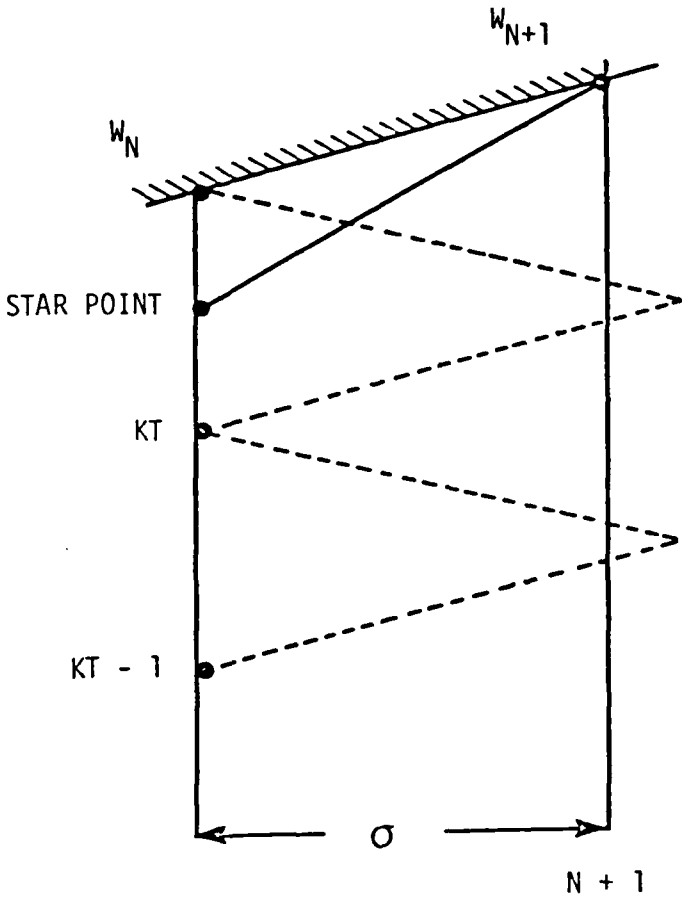

Figure 8. Wall Interaction.

equation:

$$p_{w_{n+1}} = p^*_n + \frac{\left[\tau^*_n - \tau_{w_{n+1}} + g^* \sqrt{\sigma^2 + (y_{w_{n+1}} - y^*_n)^2}\right]}{b^*_n} \qquad (57)$$

The remaining properties along the n+1 line are determined and the diffusion calculation is performed. The wall boundary conditions for the diffusion step, Eqs. (55) are imposed by inserting a data point above the wall denoted by KT+1. The numerical difference form of Eqs. (55) are then given by:

$$\begin{aligned} \alpha_{i_{KT+1}} &= \alpha_{i_{KT}} \\ H_{KT+1} &= H_{KT} \\ q_{KT+1} &= q_{KT} - \frac{c_f}{2} \frac{(\rho q)^2_{mean}}{\mu} \left(y_{KT+1} - y_{KT}\right) \end{aligned} \qquad (58)$$

where the physical location of the KT+1 point is given by:

$$y_{KT+1} = y_w - y_{KT}$$

Finally, the iterative process between the characteristic step and the diffusion step is performed as described before.

This analysis has been applied to a jet flow configuration bounded by a parallel wall. This configuration is basic to many fuel injection problems. The results for an underexpanded all-supersonic ducted jet with $P_j/P_e = 2$ and with hydrogen (primary flow) exhausting in air (secondary flow) are presented in this section; initial conditions for this calculation are given in Table 1. Two sets of calculations have been carried out; one set with a constant eddy viscosity and the second set with a viscosity computed by the two-equation TKE model. Figs. 9a through 9f show the results of the first case where $\mu = 0.00449$ lb-sec/ft^2 was chosen. This is a rather high value for the viscosity and the results reflect this fact. Figure 9a shows the wall and axis pressure distribution up to $x/r_j = 44$. The initial rise in pressure on the axis is related to the value of

TABLE 1.

INITIAL CONDITIONS FOR SAMPLE CASE				
AXISYMMETRIC HYDROGEN INJECTION INTO AIR STREAM				
Stream	Mach No.	Velocity (Ft/sec)	Pressure (LBF/Ft^2)	Temperature (^oK)
Air	3.375	8333	5290	1500
Hydrogen	2.032	16,634	10,580	1100

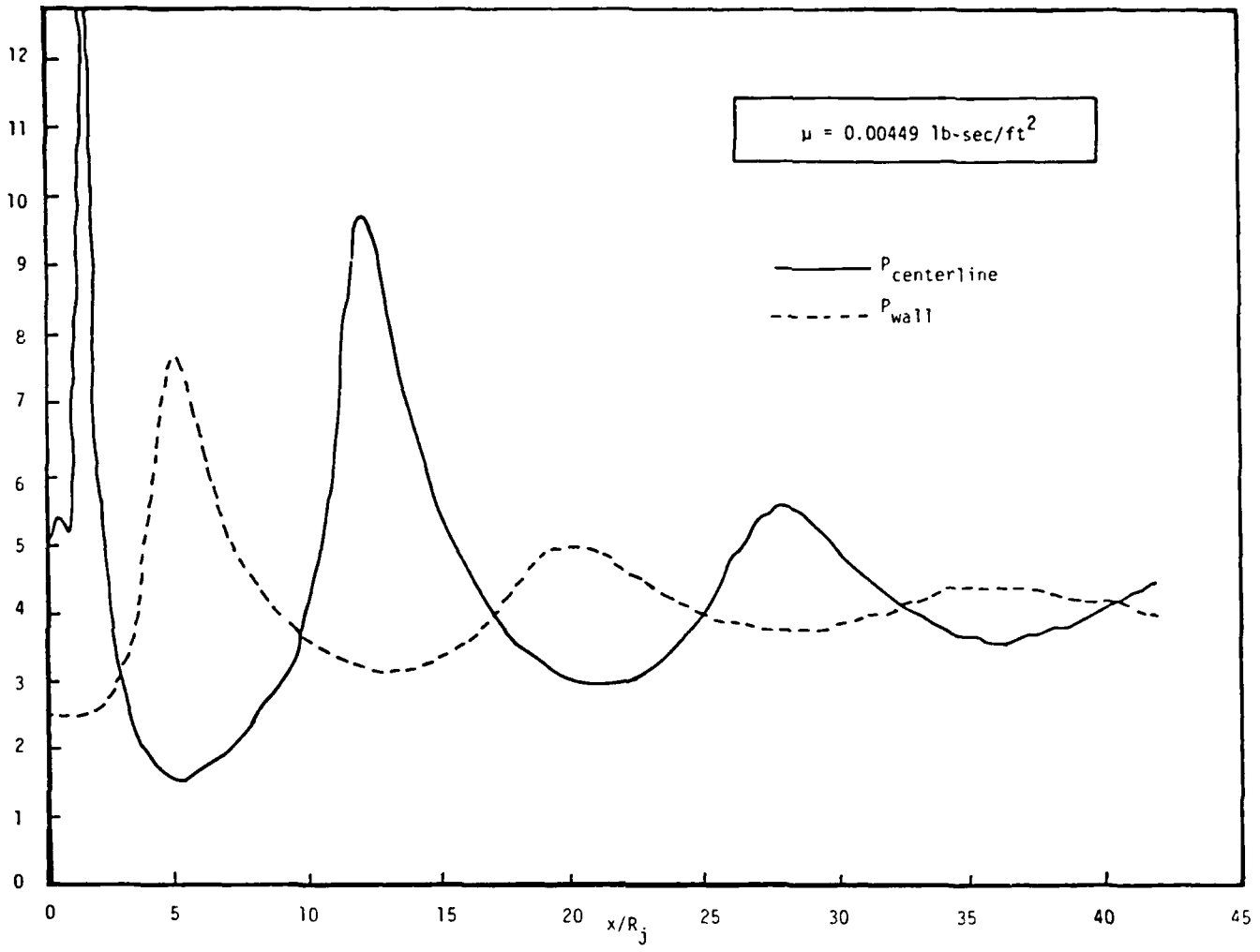

Figure 9 a. Wall and Centerline Pressure Distribution.

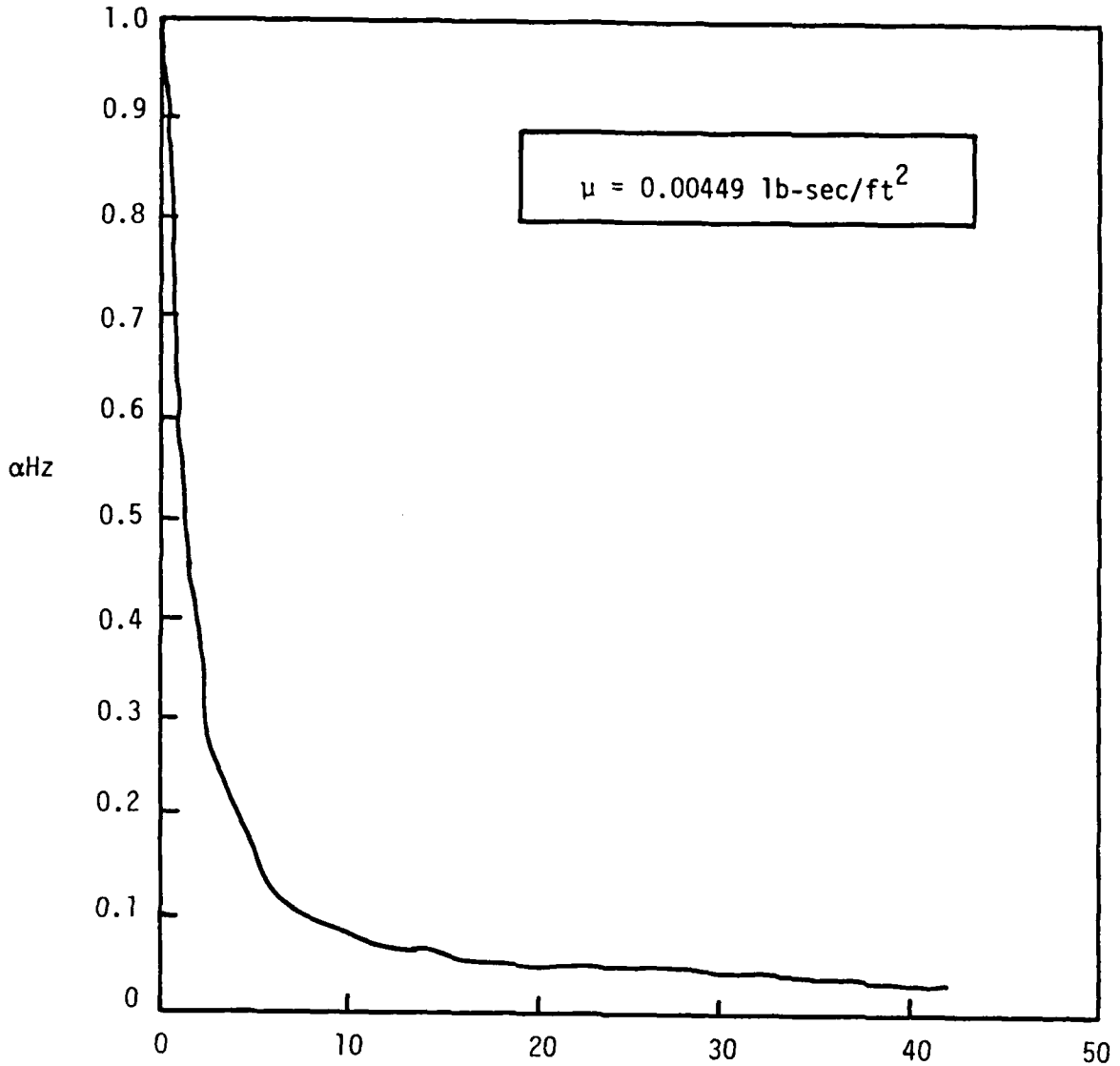

Figure 9 b. Axial Decay of Hydrogen Mass Fraction.

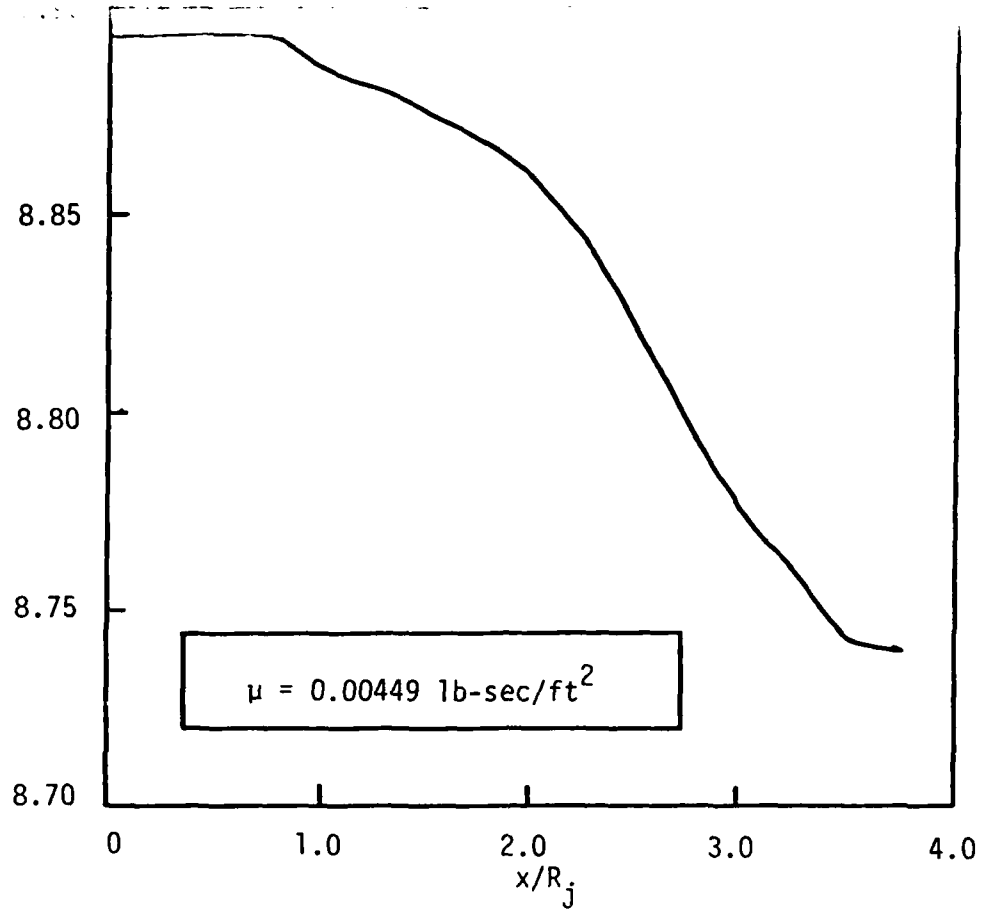

Figure 9 c. Pressure Profile at x/R_j = 40.6.

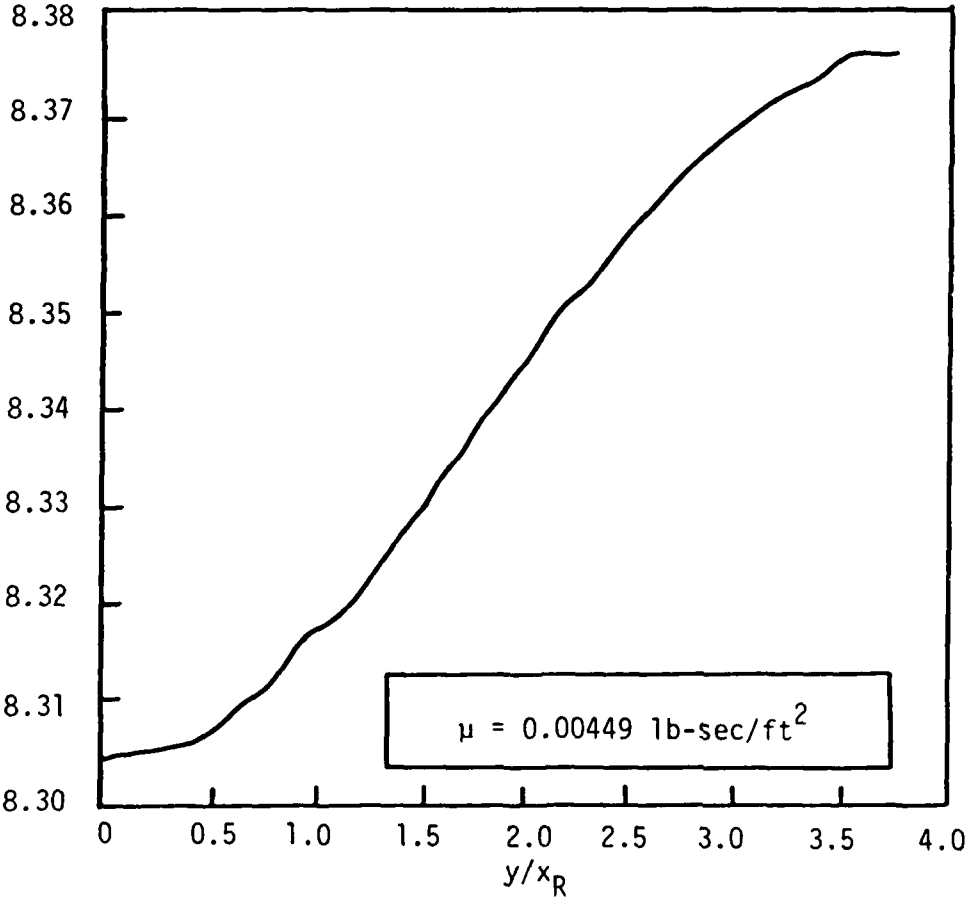

Figure 9 d. Velocity Profile at x/R_j = 40.6.

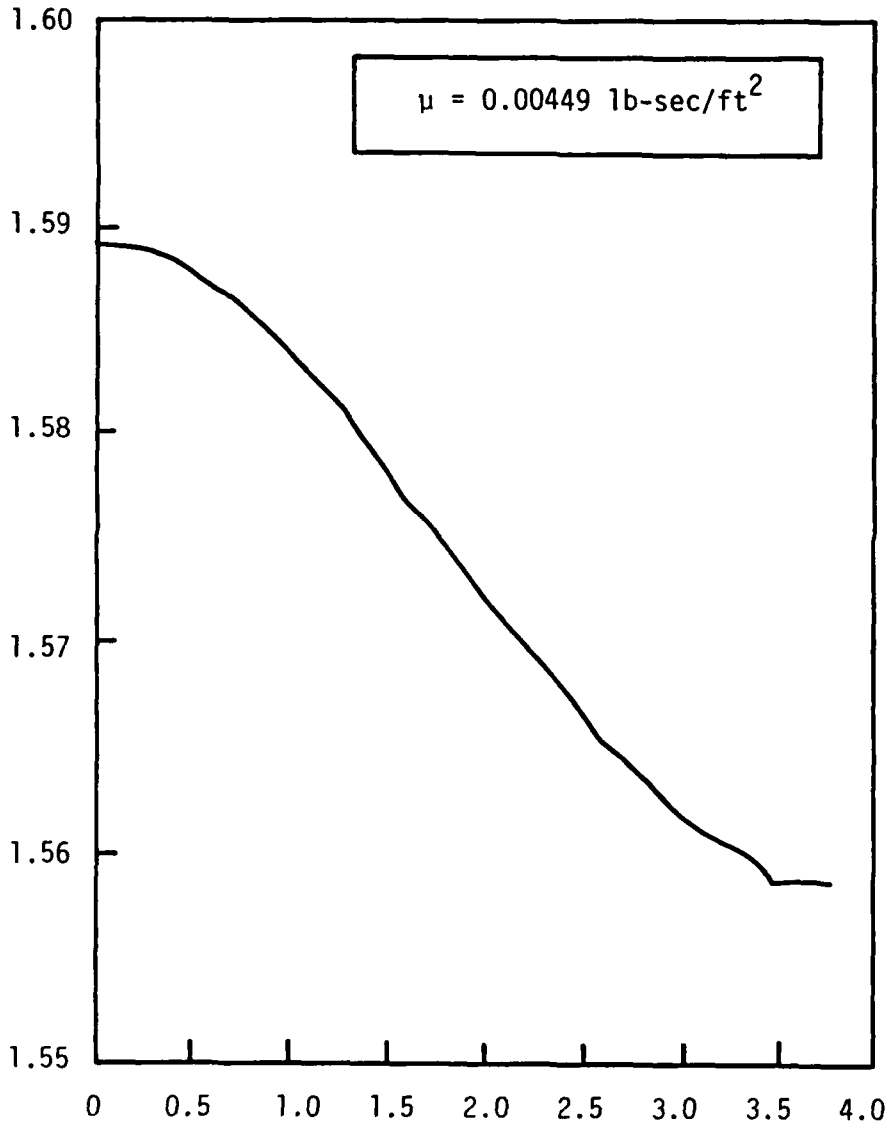

Figure 9e. Temperature Profile at x/R_j = 40.6.

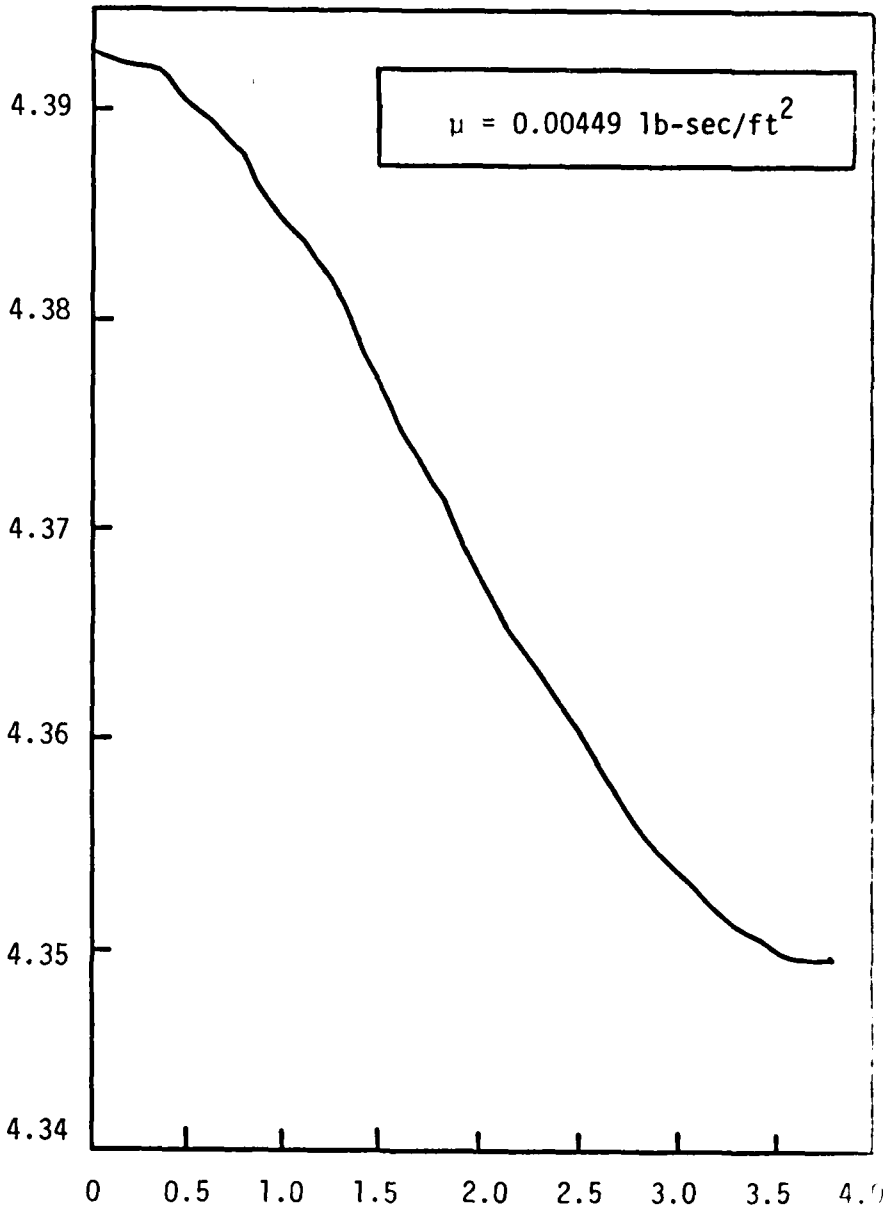

Figure 9f. Hydrogen Mass Fraction Profile at x/R_j = 40.6.

viscosity and the initial pressure ratio. Later with the adoption of the two-equation TKE model this sharp rise disappears. The axial decay of hydrogen mass fraction is shown in Fig. 9b. Because of the high viscosity the decay is almost immediate with no potential core formation. Again, later we shall show that this shortcoming is eliminated by the use of the TKE model for turbulence prescription. Figures 9c to 9f show the profiles of pressure, velocity, temperature and hydrogen mass fraction at x/r_j = 40.6, which are typical of a well mixed flowfield.

Figs. 10a to 10f represent the flowfield for similar initial conditions and geometry but with the constant viscosity replaced by the two-equation TKE model. Fig. 10a shows the distribution of wall and axis pressure. The initial sharp rise in the centerline pressure present in the previous case goes away with the adoption of this turbulence model. Fig. 10b shows the axial decay of hydrogen mass fraction. Based on this the potential core length can be estimated to be approximately 20 jet diameters. Figs. 10c to 10f show the profiles of pressure, velocity, temperature and hydrogen mass fraction at x/r_j= 38.4, which in general show that the width of the pressure field is substantially greater than the spread of the viscous region.

The results of these calculations show the possibility of the development of relatively large pressure gradients in supersonic combustor flows. The sensitivity of the induced pressure field to turbulence model assumptions is also demonstrated by these results. However, conventional turbulence modeling was used in this analysis and the direct effect of the pressure gradient on turbulence level was not included in these calculations. Furthermore, the explicit effects of pressure fluctuations on the turbulence was also neglected in these baseline calculations. These pressure coupling effects are the key elements that have been previously cited in this report as requiring inclusion in the analysis and the results of the preliminary calculations indicate that the induced pressure gradients can play a significant role in the turbulence-pressure interaction phenomenon.

Because reacting flow is the ultimate application of the research to be carried out in this program, the chemical kinetics of the reaction process must also be considered in the analysis. Short residence times and relatively low pressures such as are encountered in a scramjet, increase the importance of chemical kinetics

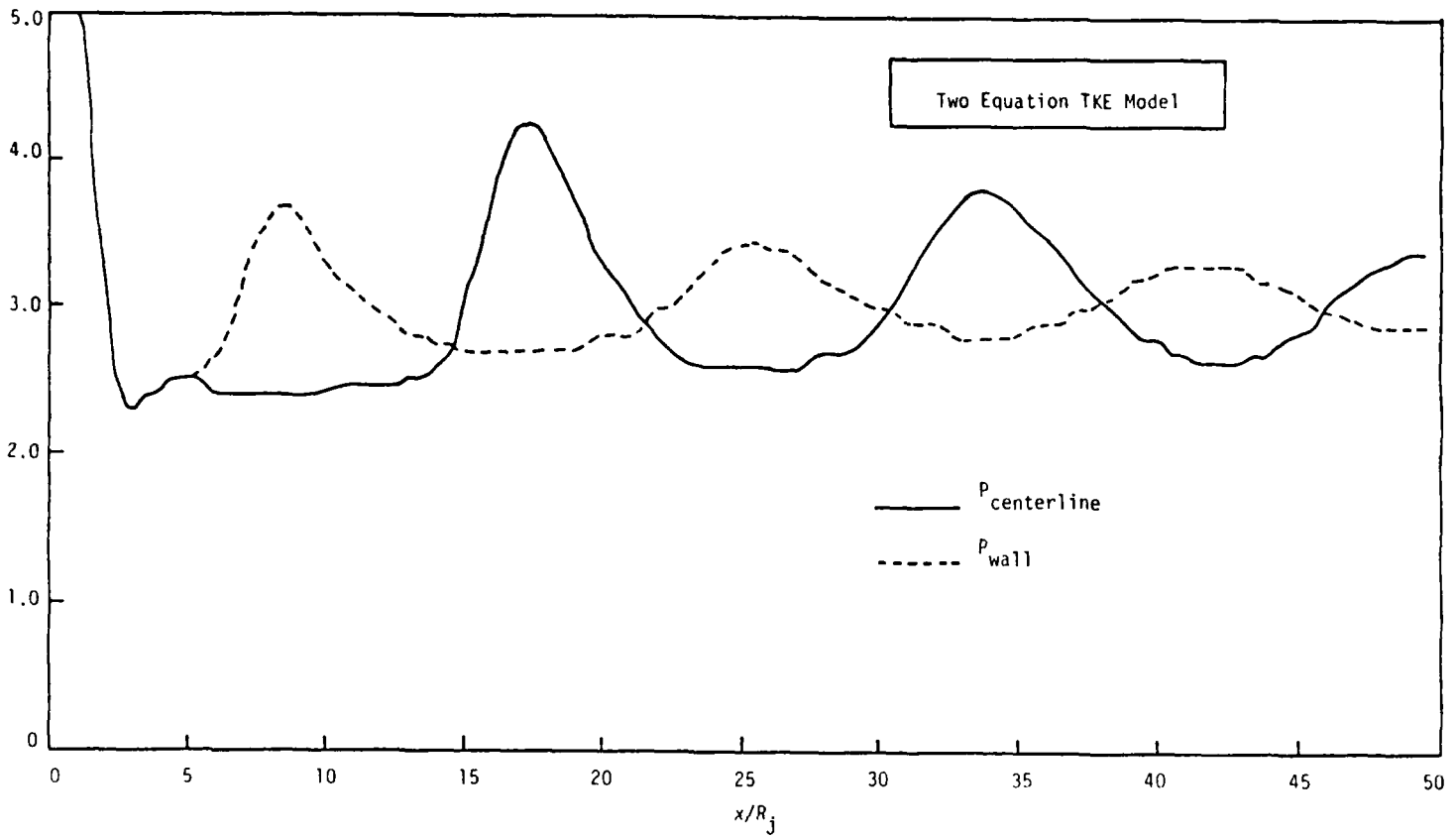

Figure 10 a. Wall and Centerline Pressure Distribution.

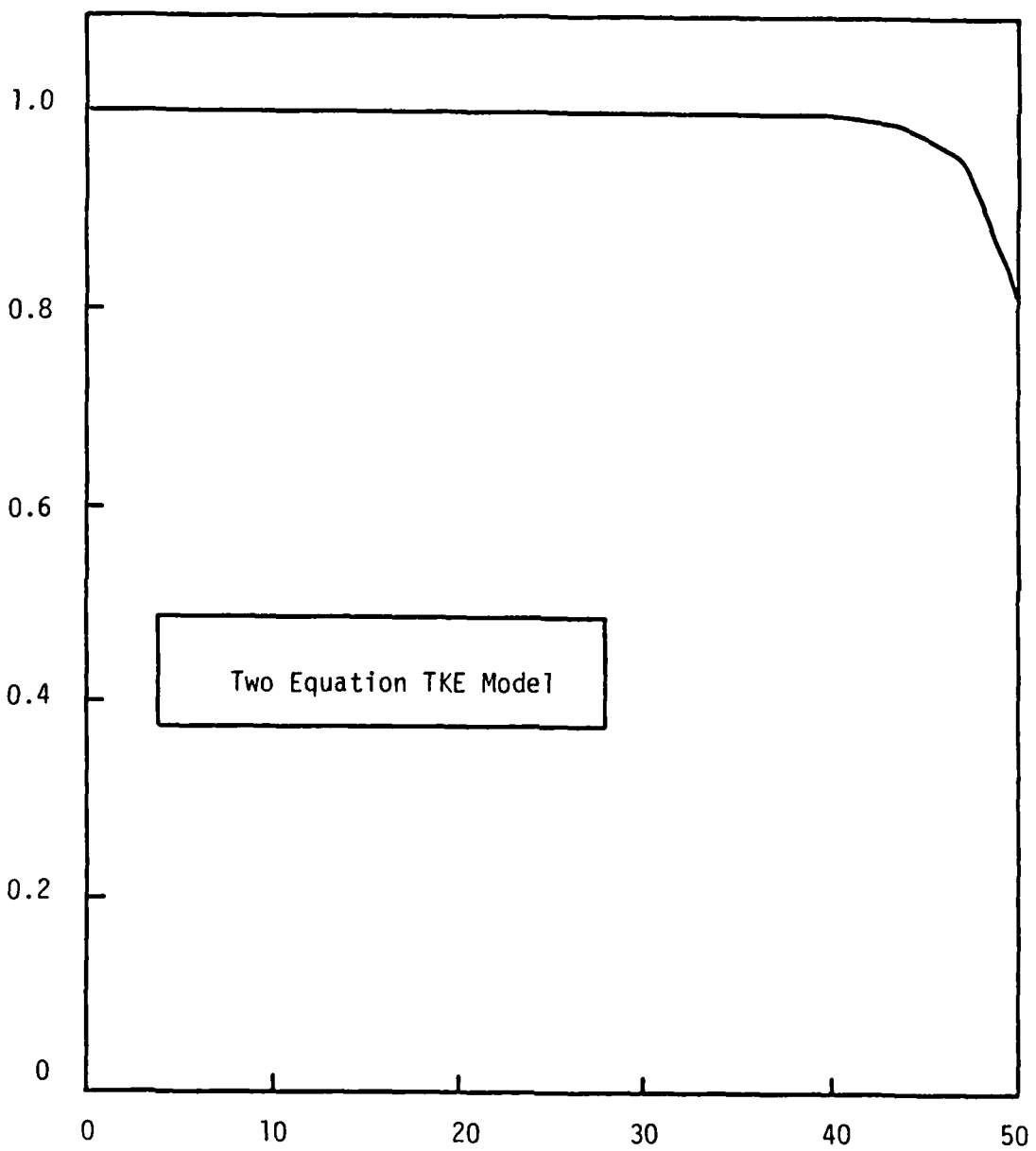

Figure 10 b. Axial Decay of Hydrogen Mass Fraction.

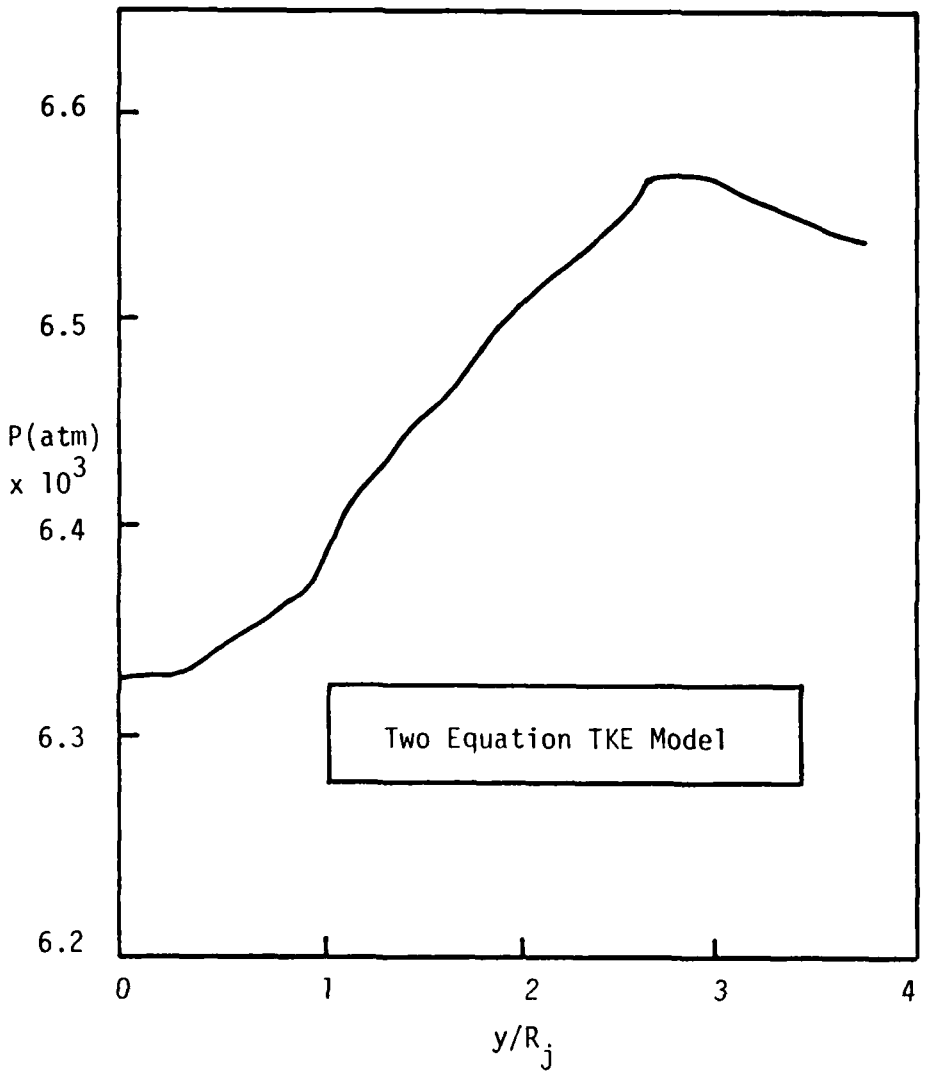

Figure 10 c. Pressure Profile at x/R_j = 38.4.

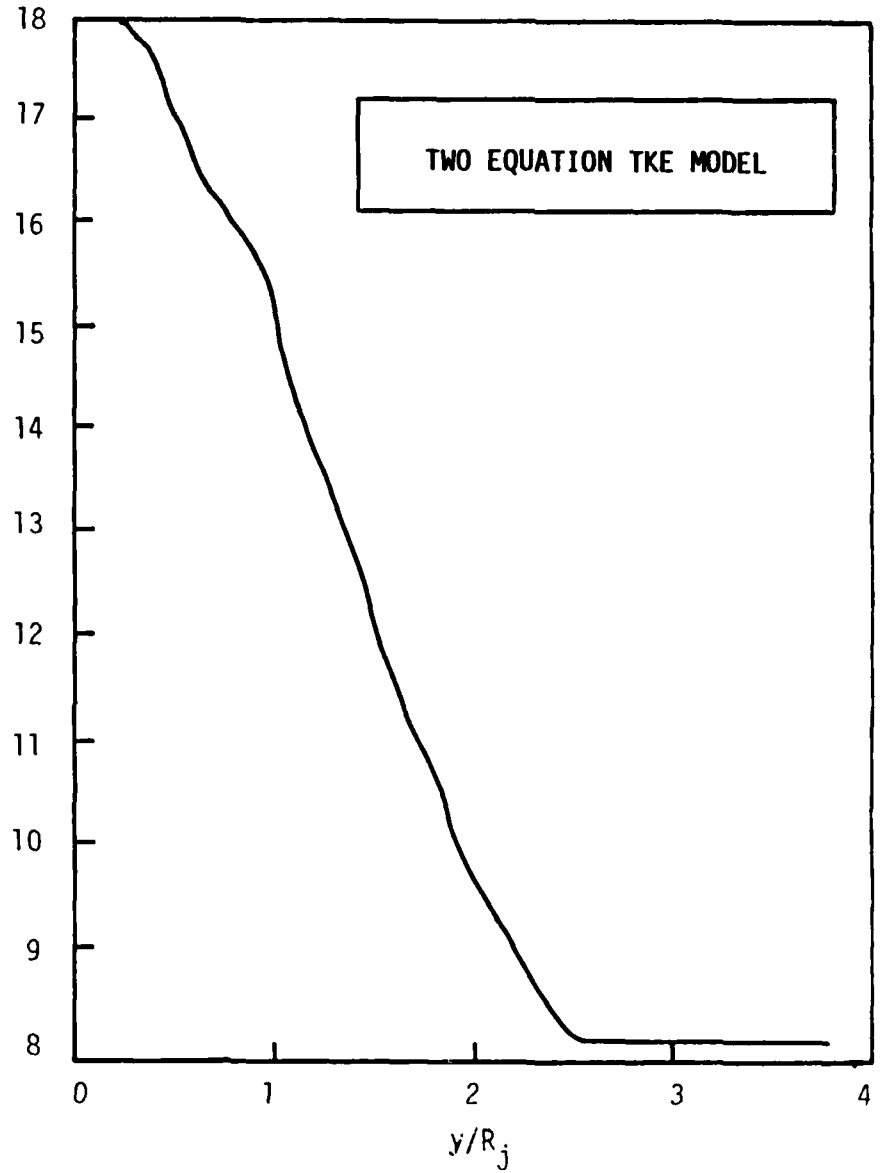

Figure 10 d. Velocity Profile at x/R_j = 38.4.

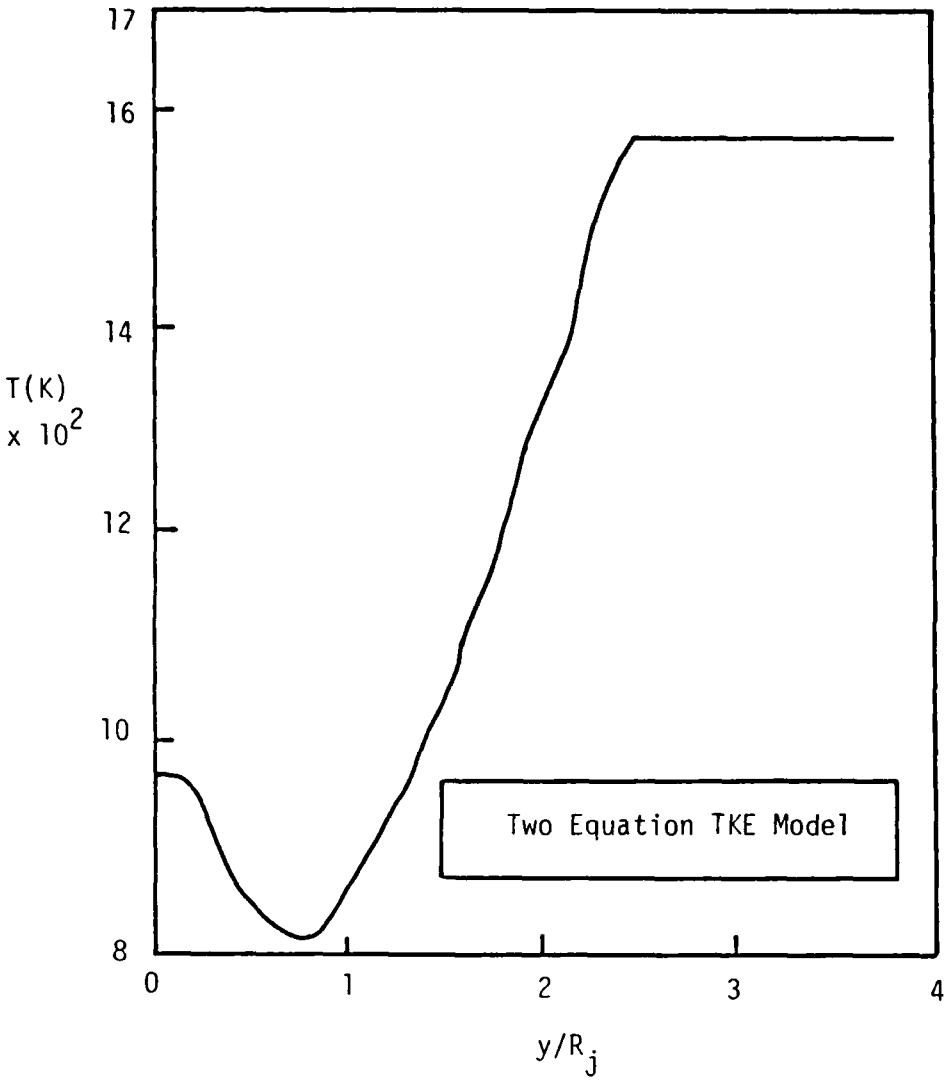

Figure 10c. Temperature Profile at x/R_j=38.4.

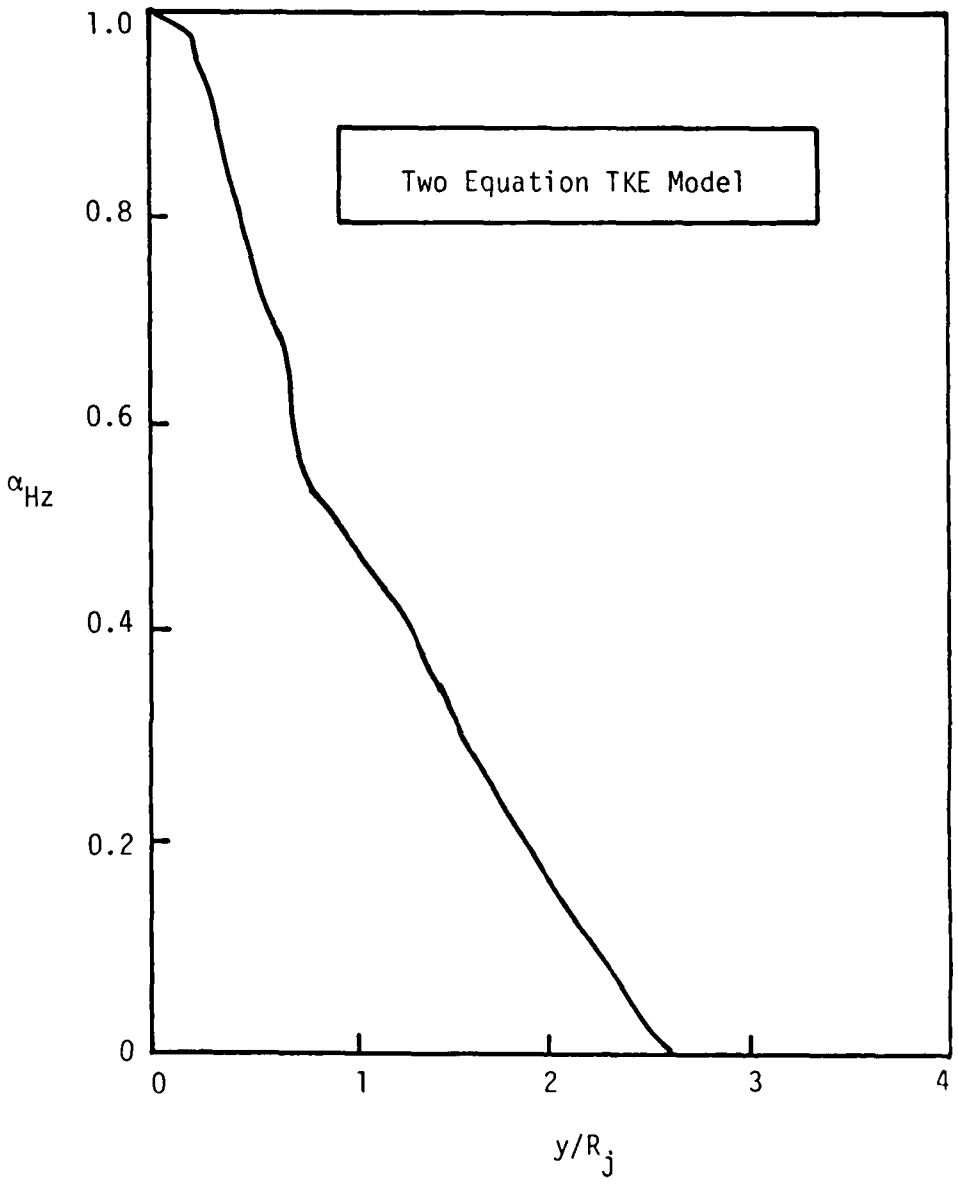

Figure 10d. Hydrogen Mass Fraction Profile at x/R_j=38.4.

effects in a scramjet relative to what is observed in subsonic combustors. At the same time, turbulence-chemistry effects also become important. The analysis of the interaction between turbulence and chemical reaction rates is a subject of considerable current interest, but no tractable approach for including a general and detailed finite-rate kinetics model in the analysis of turbulence-combustor interactions has yet been developed. Although the relatively small pressure fluctuations and pressure gradients strongly affect the turbulent kinetic energy balance their influence on chemical kinetic rates needs to be determined. Thus, as a first step in the consideration of all of the effects involved in turbulent mixing and reaction in a supersonic flow, a fast-chemistry, probability distribution function closure for the reaction problem should be used. However, stronger pressure gradients can be used to control the combustion process in a supersonic flow, and these will also affect the mixing process. Thus, an assessment of the effects of pressure gradients and pressure fluctuations in an environment where chemical kinetics effects are important must also be considered.

4.0 PROFESSIONAL PERSONNEL

The following personnel have contributed to the work conducted on this project:

Dr. R. B. Edelman

Mr. W. N. Bragg

Dr. K. T. Wu

Dr. M. Y. Bahadori

5.0 INTERACTIONS

The sudden expansion (dump) combustor work carried under the task outlined in Section 1 involves interactions with personnel in the Ramjet Technology Branch (RJT) at AFWAL/PORT, Wright-Patterson Air Force Base.

In addition, Dr. Edelman chaired the JANNAF workshop entitled "Turbulence in Ramjet Combustors" held in conjunction with the 22nd JANNAF Combustion Meeting, 7-10 October, 1985 in Pasadena, California. The objective of this workshop was to provide a link between current basic research on turbulence to problems in ramjet combustion and to foster the utilization of relevant information on turbulence in the design of ramjet systems. The discussions were largely devoted to the role of large scale structures in turbulent mixing and combustion. Both computer simulations and experimental work were presented and discussed at the workshop.

REFERENCES

1. S.F. Birch and J.M. Eggers, "A Critical Review of the Experimental Data for Developed Free Turbulent Shear Layers", Free Turbulent Shear Flows, Vol. I - Conference proceedings, NASA SP-321, 1973, pp 11-40

2. Free Turbulent Shear Flows, Vol. II - Summary of Data, NASA SP-321, 1973, P.14.

3. P.T. Harsha, "Free Turbulent Mixing: A Critical Evaluation of Theory and Experiment", AEDC-TR-71-36, February 1971.

4. G. Brown and A. Roshko, "The Effect of Density Differences on the Turbulent Mixing Layer", Turbulent Shear Flows, AGARD-CP-93, January 1972, pp. 23-1 - 23-12.

5. P.Bradshaw, "Compressible Turbulent Shear Layers", Annual Review of Fluid Mechanics, Vol. 9, 1977, pp 33-54.

6. Y.H. Oh, "Supersonic Free Turbulent Mixing Layers", Turbulent Mixing in Nonreactive and Reactive Flows, S.N.B. Murthy, ed., Plenum Press, 1975, pp 327-331.

7. O.M. Phillips, "On the Generation of Sound by Supersonic Turbulent Shear Layers", Journal of Fluid Mechanics, Vol. 9, Part 1, 1960, pp 1-28.

8. J.P. Dussuage, J. Gaviglio and A. Favre, "Density Changes and Turbulence Production in the Expansion or Compression of a Turbulent Flow at Supersonic Speed", Structure and Mechanisms of Turbulence II, H. Fiedler, ed., Lecture Notes in Physics, Vol. 76, Springer-Verlag, Berlin-Heidelberg-New York 1978, pp 385-395.

9. P.A. Libby and K.N.C. Bray, "Countergradient Diffusion in Premixed Turbulent Flames", AIAA Journal, Vol. 19, No. 2, Feb. 1981, pp 205-213.

10. W.C. Strahle and S.B.S. Chandra, "Pressure-Velocity Correlation in a Reactive Turbulent Flow", AIAA Journal, Vol. 20, No. 1, Jan. 1982, pp 129-135.

11. S.M. Correa, "Prediction of an Axisymmetric Combusting Flow", AIAA Journal, Vol. 22, No. 11, Nov. 1984, pp 1602-1610.

12. N.M.Komerath and W.C. Strahle, "Measurement of the Pressure-Velocity Correlation in Turbulent Reacting Flows", AIAA Paper 83-0400, 1983.

13. Rotta, J.C. (1979) "Eine theoretische Uutersuchung Uber den Eiufluss der Drucksherkorrelationen auf die Entwicklung driedimensionaler turbulenter Grenzschichten" DFVLR-FB-79-05, Deutsche Forschungs-und Versuchsaustad + fur Luft-und Raumfahrt.

14. Hanjalic, K., Launder, B.E., and Schiestel, R. (1979) "Multiple-Time-Scale Concepts in Turbulent Transport Modeling" Paper presented at Second Symposium on Turbulent Shear Flows.

15. Fabris, G., Harsha P.T., and Edelman, R.B. (1981) "Multiple-Scale Turbulence Modeling of Boundary Layer Flows for Scramjet Applications", NASA CR-3433.

16. Edelman, R., and G. Wilerstein., "Mixing and Combustion in Supersonic Flow with Lateral Pressure Gradient Effects", GASL TR No. 636, August 1968.

END

11-86

DTIC